THERMAL TRANSIENT TESTING USING TDS TECHNIQUE

BY

NYAME MICHAEL

RECOMMENDED:

Prof. Djebbar Tiab – Committee Chair

Dr. Alpheus Igbokoyi – Committee Member

Prof. Sam Osisanya – Committee Member

APPROVED:

Chair, Department of Petroleum Engineering

Academic Provost

Date

THERMAL TRANSIENT TESTING USING TDS TECHNIQUE

A

THESIS

Presented to the Faculty of the African University of Science and Technology

In Partial Fulfillment of the Requirement for the Degree of

MASTER OF SCIENCE

By

NYAME MICHAEL

Abuja, Nigeria

December, 2011

Abstract

In the estimation of most reservoir parameters in well test, the reservoir is assumed to be isothermal which is practically not true due to the fact that there are heat sources due to friction in the wellbore, works done by the drill bit and in thermal recovery. Although, this temperature change is small, it can serve other beneficial purposes in the reservoir and wellbore. The research work used the temperature change to estimate permeability, skin factor and initial temperature of the reservoir. This work brought out equations to be used in the estimation these reservoir parameters and the applied to field data. These results obtained compared with the true reservoir parameters of field data were almost the same especially the permeability and initial reservoir temperature although the same could not be said about the skin factor since that of the estimated and true value were quite different. This research work brought out the idea that thermal transient testing can be used as a tool for estimating some reservoir parameters or as verification for estimated parameters using other well test methods. This research work also generated type curve for dimensionless temperature derivative versus shut-in time for different skin factors (damaged, neither damaged nor stimulation and stimulation) as well as type curve for dimensionless temperature derivatives versus shut-in time for different dimensionless radii with their respective behaviors.

DEDICATION

This research work is dedicated to;

God Almighty - The author and finisher of my destiny. You lifted me from the dunghill and established me in heavenly places……

My Sweet Mum – Victoria Nyann, You are my heroine. You are a phenomenon. Your strength, tenacity and determination put you in a class of your own…….

Gladys Acquah – My dear friend, how could l have done it with you. I love so much…….

My siblings – Eric, Linda, Beatrice and Eunice. You guys are so wonderful…….

ACKNOWLEDGEMENT

I thank the Almighty for the strength, inspiration, guidance, and other provisions which have ensured the success of this research work– Glory to the Jehovah Nissi forever and ever.

I also express my gratitude to Professor Djebbar Tiab for the immense supervision of this work. Your fruitful effort and time spent on this thesis has gone a long way to add quality to it – thank you very much.

Thirdly, my appreciation goes to my committee members; Dr. Alpheus Igbokoyi and Prof. Sam Osisanya for the timely help they provided in editing the work. Also, I thank all petroleum faculty members of AUST who have assisted by raising me up academically to be able to carry out this work. The contributions you have made as far as this research is concern are deeply recognized.

I extend a hand of gratitude to my mum Victoria Nyann for her love, care and sponsorship throughout education. I also extend my appreciation to my siblings, Eric, Linda, Beatrice and Eunice for their support and prayers. I also extend my appreciation to other colleagues of mine including Titus Ntow-Ofei, for their encouragement, criticism and concern. Your support no matter how small it is has been significant to the success of this research work – thank you all.

Lastly, I extend a hand of gratitude to the love of my life, Gladys Akosua Gyamfuah Acquah, whose contribution to my attainment of this enormous feel cannot be quantified. Honey l love you.

Table of Contents

Contents		Page
Signature Page		**i**
Title Page		**ii**
Abstract		**iii**
Dedication		**iv**
Acknowledgements		**v**
Table of Contents		**vi**
List of Figures		**ix**
List of Tables		**x**
Chapter One – Introduction		**1**
1.1	Introduction.	1
1.2	Statement of Problem.	1
1.3	Objectives.	2
1.4	Scope of Work.	2
Chapter Two – Literature Survey		**3**
2.1	Introduction.	3
2.2	Pressure transient testing.	3
2.3	Pressure Drawdown Test.	**5**
2.4	Pressure Build-up Test.	**5**
2.5	Pressure Derivative.	**6**
2.6	TDS Technique.	**8**
	2.6.1 The Mathematical Model.	**8**
	2.6.2 A step-by-step procedure for the basic case (Tiab, 1995). .	**11**
2.7	Temperature disturbance in a Well..	12
2.8	Thermal Effect on gas wells..	13

Chapter Three – Derivation of Relevant Equation **15**

3.1 Introduction. 15

3.2 Mathematical Model.. 15

3.2.1 Derivation of any expression for permeability. . . . 17

3.2.2 Derivation of any expression for skin. 19

3.3 Applying TDS technique to thermal transient. 20

3.4 Equations extended to real gases. 22

3.4.1 Considering the Van Der Waals forces. 23

3.4.2 Pseudo Reduced Temperature function. 24

3.5 Developing type curves from dimensionless temperature and time functions for different r_D.. 25

3.6 Developing type curves from dimensionless temperature and time functions for different skin factors. 27

CHAPTER FOUR – Application of Equations to Field Data **28**

4.1 Introduction. 28

4.1.1 Estimating the Permeability using Semi-log thermal transient. . 32

4.1.2 Estimating the skin using Semi-log thermal transient. . . 33

4.2 Applying the TDS technique to the temperature data. . . . 33

4.2.1 Estimating the permeability using TDS thermal transient. . 36

4.2.2 Estimating the skin using TDS thermal transient. . . . 37

4.3 By applying this Pseudo Reduced Temperature function. . . 37

CHAPTER FIVE – Discussions of Results **42**

5.1 Discussion of results conventional thermal transient and thermal transient using TDS technique. 42

5.2 Benefits of thermal transient test over Pressure transient test. . . 45

5.2 Discussion of results of the real pseudo reduced temperature functions. 46

5.3 Discussion of type curves generated for the dimensionless Temperature derivative for different dimensionless radii. . . 47

5.4 Discussion of type curves generated for the dimensionless temperature derivative for different skin factors. 49

CHAPTER SIX – Conclusion and Recommendations 51

6.1 Conclusion. 51

6.2 Recommendations. 51

REFERENCES 53

NOMENCLATURE 56

APPENDIX A: Dimensionless Temperature data for varying dimensionless radii. 57

APPENDIX B: Dimensionless Temperature data for varying skin factors. 58

List of Figures

Figure		Page
2.1	A graph of pressure drop and its derivative versus time . . .	10
4.1	A graph of temperature drop versus shut in time	32
4.2	A graph of t*ΔT versus shut in time (unsmoothed) . . .	35
4.3	A graph of t*ΔT versus shut in time (smoothed)	36
4.4	A graph of pseudo reduced temperature drop versus shut in time. .	40
5.1	Type curve of dimensionless temperature derivatives for varying dimensionless radius	46
5.2	Type curve of dimensionless temperature derivatives for Varying skin factors..	48

List of Tables

Table		Page
2.1	Parameters obtained from well testing (Kamal, Freyder and Murray, 1995).	4
4.1	Reservoir field data.	29
4.2	Temperature data for conventional thermal transient.	30
4.3	Temperature data for TDS thermal transient.	33
4.3	Temperature data for pseudo temperature function.	38
5.1	Comparison of conventional and TDS methods of thermal transient. .	43
5.2	Comparison of conventional and TDS methods of thermal transient. .	44

CHAPTER ONE
GENERAL INTRODUCTION

1.1 Introduction

The effects of pressure transient in fluids at near-wellbore, homogenous and reservoir boundary regions have been studied extensively. Important reservoir parameters like permeability, skin factor, porosity, reserves, pressure drop, pressure drop due to skin, wellbore radius, productivity index, flow efficiency, damage ratio, wellbore storage, pore volume and drainage area have all been estimated using pressure transient testing. These reservoir parameters have been estimated with the assumption that change in temperature is relatively small and hence considered to be negligible in fluid flow. This isothermal assumption used in the estimation of these reservoir parameters, is not entire true. This is due to the fact that there are heat sources due to friction in the wellbore as well as works done by the drill bit (Marshall et al 1992). The understanding of thermal transient effect will help in better analysis of the reservoir or well to effectively maximize production rates. It will also help in the management and optimization of the reservoir. This will also help in planning the type of drilling methods, drive mechanism and production schemes to effectively maximum production. Also, thermal transient is more ideal for certain recovery processes like steam injection and in situ combustion since the heat produced or injected can be used in the thermal transient test analysis.

1.2 Statement of Problem

It has generally been assumed that fluid flow in near-wellbore, homogenous and reservoir boundary regions is generally isothermal. This assumption is not true since there is temperature change as fluid flow in the reservoir or wellbore especially in deep and thick reservoirs. Although the effects of temperature change maybe very small, it can be used to the benefit of the reservoir engineer in the estimation of the essential parameters such permeability and skin factor. There are other useful information about the reservoir which can be derived from thermal transient test such as generation of type curves, dimensionless temperature functions and pseudo

reduced temperature functions. Surprisingly, these reservoir properties have totally been neglected. This research work seeks to analysis the effect of the temperature change on the estimation of reservoir parameters using the Tiab's Direct Synthesis (TDS) technique. This technique is also extended to gas reservoirs using real pseudo reduced temperature functions to get a better understand thermal transient in gases.

1.3 Objectives

The objectives of this thesis work are;

a. To apply TDS technique to thermal transient testing to estimate reservoir parameter such as permeability and skin factor.
b. To apply thermal transient to gas reservoirs using real pseudo reduced temperature functions to estimate initial reservoir temperature.
c. To generate type curves for the dimensionless temperature and its derivatives for varying dimensionless radii.
d. To generate type curves for the dimensionless temperature derivatives for varying skin factors.

1.4 Scope of Work

Chapter one of this thesis work captures a general introduction to this research whiles chapter two reviews relevant literature of thermal transient testing. The derivation of relevant equations using the TDS technique to analyze thermal transient test will be discussed chapter three. These equations will be applied to reservoir field data in chapter four of this research work. Chapter five captures the discussion of the results obtained in chapter four. This work finally ends with the conclusions and recommendation in chapter six.

CHAPTER TWO

LITERATURE SURVEY

2.1 Introduction

Thermal transient testing is a test in which we generate and measure temperature changes in a well as a function of time. This is used in the analysis a wellbore or a reservoir. Thermal transient can therefore be used to estimate some reservoir properties like permeability and skin factor. Unlike pressure transient testing, thermal transient testing has not thorough been investigated. In pressure transient test, pressure changes are observed and measured in a well as a function of time. This pressure measurement response can be used to determine important reservoir properties.

2.2 Pressure transient Testing

A pressure transient is a pressure change in a reservoir as a result of change in equilibrium of reservoir conditions. It has been applied to Darcy and non-Darcy flows in other to effectively interpret linear, radial, and spherical flow. Radial flow is the most widely used in field applications. Most often, the external boundary conditions are difficult to estimate in field applications (Roger et al, 1966). Pressure transient can be divided into single well and multi-wells transient testing. Single well test includes pressure buildup, drawdown, injectivity and fall-off test. These tests are used for the determination of pressure responses in other to estimate reservoir properties such as reservoir behavior, permeability, skin factor, nearby boundaries, reservoir limits, reservoir boundaries, average reservoir pressure, fracture length, transmissivity, storativity, porosity and location of front boundaries. Interference, multi-rate deliverability and pulse tests are also conducted in multi-wells used to estimate properties in a region entered along a line connecting pairs of wells. Most of these tests produce similar results although certain techniques have proven to be more reliable (Lee et al, 1996). The accumulation of data from pressure transient throughout the producing life of the well gives a better understanding of the wellbore and the reservoir at large. It can help in better estimation of recoverable reserves and

permeability of the reservoir. Parameter obtained from these test are shown in table 2.1.

Table 2.1 Parameters obtained from well testing (Kamal, Freyder and Murray, 1995)

Types of test	Derived reservoir parameter
Drill stem test	Reservoir behavior, permeability, skin, nearby boundary, reservoir pressure
Draw down test	Reservoir behavior, permeability, skin, fracture length, reservoir limits and boundaries
Buildup test	Average Reservoir pressure , permeability, skin, nearby boundary, reservoir boundaries
Interference and pulse test	Communication between wells, transmissivity, porosity, storativity, interwell permeability, vertical permeability
Layered reservoir test	Properties of individual layers, outer boundaries, horizontal permeability, vertical permeability, average layered pressure.
Fall-off test	Mobility in various banks, Average Reservoir pressure, skin, fracture length, location of front boundaries.
Step-rate test	Formation parting pressure permeability, skin
Repeat-multiple- formation test	Pressure profile

2.3 Pressure Drawdown Test

A Pressure Drawdown Test involves the measuring of the change in bottom hole pressure in the production life of wellbore at specified time. Pressure Drawdown Test is normally started at shut-in time and the rate increased steadily. This makes new wells perfect for drawdown test since they are mostly in shut-in-state with uniform reservoir pressure. Although, the production rate in drawdown pressure measurement is not constant, the choke setting is kept constant. The constant choke setting results in drop of the production rate in the wellbore. When the choke setting is adjusted to give a constant production rate, transient state results which affect data accumulated from the wellbore (Chad, 2009).

2.4 Pressure Build-up Test

Pressure buildup testing involves the production of a well at constant production rate for some specified time and then shutting the well in at the surface. The pressure is then allowed to build up in the wellbore and then down-hole pressure in the wellbore at each time step is recorded. The recorded data can then aid in the estimation of reservoir properties like formation permeability, formation damage or stimulation, drainage area and reservoir boundaries. It can helps in understanding the heterogeneity in the wellbore or reservoir. In order to effectively estimate the these reservoir parameters, the surface and subsurface mechanical conditions such as casing sizes, well depth, packer condition must be clearly defined (Amanat, 2009). Pressure buildup test are easily run on gas well. Most often the reservoir properties such permeability, formation damage and average reservoir pressure are easily estimated one's the effects of wellbore storage is determined. Normally, the drawdown test is followed by buildup test. The drawdown begins from a stabilized reservoir condition represented by the stabilized reservoir pressure. The data recorded from buildup test are directly affected by this drawdown. The basic equations used in pressure transient test are derived from the diffusivity equation;

$$\frac{1}{r}\frac{\partial}{\partial r}\left(r\frac{\partial P}{\partial r}\right)=\frac{1}{\alpha}\frac{\partial P}{\partial t} \tag{2.4.1}$$

$$P(r,t) = P_i + \frac{70.6qB\mu}{kh} Ei\left(\frac{948\emptyset\mu c_t r^2}{kt}\right) \tag{2.4.2}$$

$$P(r,t) = P_i - \frac{162.6qB\mu}{kh}\left[log\left(\frac{kt}{\emptyset\mu c_t r^2}\right) - 3.23\right] \tag{2.4.3}$$

$$P_{wf} = P_i - \frac{162.6qB\mu}{kh}\left[log\left(\frac{kt}{\emptyset\mu c_t r^2}\right) - 3.23\right] \tag{2.4.4}$$

A semi log plot of P_{wf}, versus t gives a straight line portion of slope, m. This line corresponds to the time the pressure transient behaves as if the reservoir were infinite. The slope is used to calculate the reservoir permeability.

$$slope, m = -\frac{162.6qB\mu}{kh} \tag{2.4.5}$$

therefore

$$permeability, k = -\frac{162.6qB\mu}{hm} \tag{2.4.6}$$

2.5 Pressure Derivative

This work was done by Tiab (1975) to use the derivative method to analyze and estimate reservoir parameters. In this study, the continuous line source solution method and differentiation under the integral sign by the use of Leibnitz' Rule. The basic equations used by Tiab in his research are as follows;

$$F(\alpha) = \int_{a(\alpha)}^{b(\alpha)} \psi(x,\alpha)\ dx \tag{2.5.1}$$

Taking the derivative of equation 2.5.1 where a and b are differentiable functions of α and where $\psi(x,\alpha)$ and $\partial\psi/\partial\alpha$ continuous in x and a, then:

$$\frac{\partial F}{\partial \alpha} = \int_{a(\alpha)}^{b(\alpha)} \frac{\partial \psi(x,\alpha)}{\partial \alpha}\ dx + \psi(b(\alpha),\alpha)\frac{db(\alpha)}{d\alpha} - \psi(a(\alpha),\alpha)\frac{da(\alpha)}{d\alpha} \tag{2.5.2}$$

Equation 2.5.2 can be re-written as

$$\frac{\partial[P(r_D,t_D)]}{\partial t_D} = P_D^{'} = \frac{1}{2}\frac{\partial}{\partial t_D}\left[\int_x^{\infty}\frac{e^{-u}}{u}\,du\right] \tag{2.5.3}$$

Applying Leibnitz' Rule to equation 2.5.3 gives;

$$\frac{\partial P_D}{\partial t_D} = P_D^{'} = \frac{1}{2}\left(-\frac{e^{-X}}{X}\right)\frac{\partial X}{\partial t_D} \tag{2.5.4}$$

where

$$X = \frac{r_D^2}{4t_D}$$

Therefore substituting equation 2.11 into 2.8 gives;

$$P_D^{'} = -\frac{1}{2}\left(\frac{4t_D}{r_D^2}\right)\left[\frac{r_D^2}{4t_D}\left(-\frac{1}{t_D^2}\right)\right]exp\left(-\frac{r_D^2}{4t_D}\right) \tag{2.5.5}$$

Equation 2.5.5 therefore become

$$P_D^{'} = \frac{1}{2t_D}exp\left(-\frac{r_D^2}{4t_D}\right) \tag{2.5.6}$$

For r_D=1, and t_D>250 results to

$$exp\left(-\frac{r_D^2}{4t_D}\right) \approx 1$$

Therefore equation 2.5.6 becomes:

$$P_{wD}^{'} = \frac{1}{2t_D} \tag{2.5.7}$$

Taking the logarithm of both sides of equation 2.5.7 results in:

$$logP_{wD}^{'} = -logt_D - 0.30103 \tag{2.5.8}$$

A log log plot of P'_{wD} versus t_D gives a straight line of slope -1 during the infinite-acting portion of the curve. Equation 3.4 can also be expressed as:

$$t_D \times P_{wD}^{'} = \frac{1}{2} \tag{2.5.9}$$

This equation indicates that a log log plot of t_D x P'_D versus t_D yields a horizontal straight line during the infinite-acting portion of the curve. Equation 2.5.6 can also be expressed as:

$$P_D^{'} \times r_D^2 = \frac{1}{2(t_D/r_D^2)} exp\left(-\frac{1}{4(t_D/r_D^2)}\right) \quad (2.5.10)$$

2.6 TDS Technique

This technique is referred to as the Tiab's Direct Synthesis (TDS) Technique. It is a technique developed by Tiab's research work in 1993. This was used for the estimation of reservoir and well parameters without type-curve matching. It involves the use of log-log plots of the pressure and pressure derivative versus time to estimate these reservoir parameters. It is applicable to the interpretation of pressure buildup and drawdown tests. The TDS technique gives more accurate results in estimating permeability, skin, and wellbore storage compared to the use of type curves and pressure derivatives. This technique was applied to different cases of reservoir conditions such as;

- Unit slope and infinite acting lines are observed (Basic case)
- The early-time unit slope line is not observed
- The infinite acting line is not observed (Short test)
- The unit-slope line and the peak are not observed (No wellbore storage)
- The unit slope and infinite acting lines have not been observed.

2.6.1 The Mathematical Model

dimensionless pressure, $P_D = \left(\frac{kh}{141.2q\mu B}\right)\Delta P$ (2.6.1)

dimensionless time, $t_D = \left(\frac{0.0002637k}{\phi c_t \mu r_w^2}\right)t$ (2.6.2)

dimensionless wellbore storage coefficient , $C_D = \left(\frac{0.8935}{\phi c_t h r_w^2}\right)C$ (2.6.3)

A log log plot of P'_{wD} versus t_D gives a straight line of slope 1 during early time. This line corresponds to pure wellbore storage flow. This equation of this straight line is:

$$P_D = \frac{t_D}{C_D} \tag{2.6.4}$$

Combining equation 2.6.2 and 2.6.3 results to:

$$\frac{t_D}{C_D} = \left(2.95 \times 10^{-4} \frac{kh}{\mu}\right) \frac{t}{C} \tag{2.6.5}$$

Substituting equation 2.6.5 into equation 2.6.1 and solving for the wellbore storage coefficient, C

$$C = \left(\frac{qB}{24}\right) \frac{t}{\Delta P} \tag{2.6.6}$$

Where ΔP is P_i-P_{wf} for drawdown and P_{ws}-P_{wf} (Δt=0) for buildup

The pressure derivative curve also has an early time straight line of unit slope. The equation of this line is obtained by taking the derivative of equations 2.6.4 with respect to the natural log of t_D/ C_D, therefore

$$\left(\frac{t_D}{C_D}\right) P'_D = \frac{t_D}{C_D} \tag{2.6.7}$$

But dimensionless pressure derivative given by:

$$P'_D = \left(\frac{26.856 \phi c_t h r_w^2}{qB}\right) \Delta P' \tag{2.6.8}$$

The left-hand of equations side of equation 2.6.8 can be expressed in real units by combining equation 2.6.5 and 2.6.8

$$\left(\frac{t_D}{C_D}\right) P_D = \left(\frac{kh}{141.2 q \mu B}\right) (t \times \Delta P') \tag{2.6.9}$$

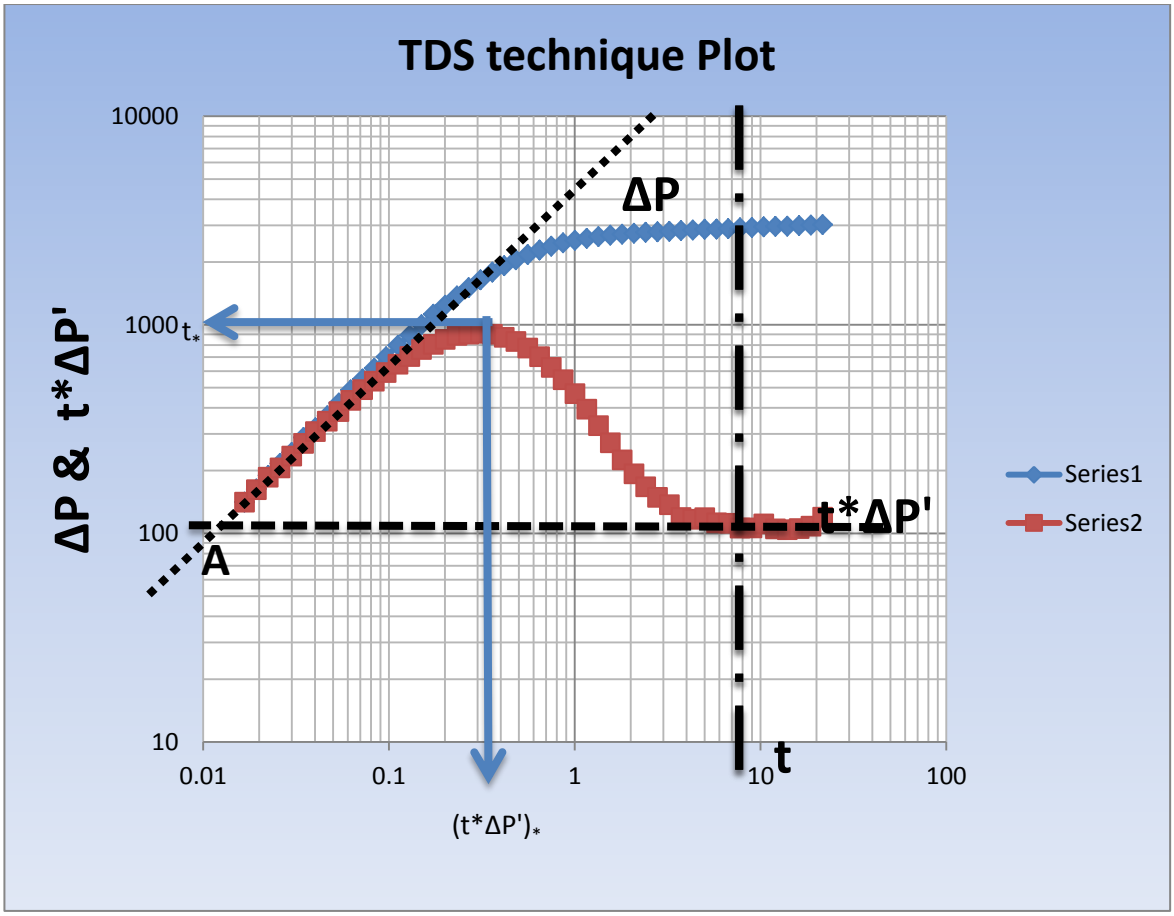

Fig. 2.1 A graph of pressure drop and its derivative versus time

From Fig 2.1 that the early time unit slope line is the same for pressure drop and pressure derivatives curves.

Also combining equation 2.6.7, 2.6.8 and 2.6.9 and solving for C we obtain an equation similar to equation 2.6.6 where ΔP is replaced with txΔP'.

$$C = \left(\frac{qB}{24}\right)\frac{t}{(t \times \Delta P')} \tag{2.6.10}$$

The infinite-acting radial flow portion of the pressure derivative is a horizontal straight line. For a homogenous reservoir, the equation of this line is:

$$\left(\frac{t_D}{C_D}\right)P_D = 0.5 \tag{2.6.11}$$

Combining equation 2.13 and 2.14 and solving for the permeability gives

$$k = \frac{70.6qB\mu}{h(t \times \Delta P')_r} \tag{2.6.12}$$

Where the subscript, *r*, stands for radial flow line.

$$m = 2.303(t \times \Delta P')_r \tag{2.6.13}$$

In order for the conventional semi log analysis and the TDS technique to yield the same value of k, equation 2.2.14a must be true.

In terms of dimensionless pressure, the equation corresponding to the radial flow line is:

$$P_{Dr} = 0.5\left[ln\left(\left(\frac{t_D}{C_D}\right)_r\right) + 80907 + ln(C_D e^{2s})\right] \tag{2.6.14}$$

An expression relating the infinite-acting radial flow line portions of the pressure and pressure derivative curves can be derived by dividing Eq. 2.2.15 with Eq. 2.2.13:

$$\frac{P_{Dr}}{\left[\left(\frac{t_D}{C_D}\right)P'_D\right]_r} = lnt_{Dr} + 2s + 80907 \tag{2.6.15}$$

Combining equations 2.2.4, 2.2.8 and 2.2.12 with Eq. 2.2.16 and solving for skin gives

$$s = 0.5\left[\frac{\Delta P_r}{(t \times \Delta P')_r} ln\left(\frac{kt_r}{\phi c_t h r_w^2}\right) + 7.43\right] \tag{2.6.16}$$

where tr is any convenient time during the infinite-acting radial flow line and ΔPr is the value of ΔP corresponding to tr.

The time of intersection of the unit-slope and infinite-acting straight lines is given by

$$t_i = \frac{1695\mu C}{kh} \tag{2.6.17}$$

2.6.2 A step-by-step procedure for the basic case (Tiab, 1995)

1. A plot of ΔP and t×ΔP' versus time is done on a log-log graph.
2. A unit-slope line corresponding to the wellbore storage flow regime is drawn using early time pressure and pressure derivative points. If there is too much noise in the derivative values, it can be drawn using only pressure points.

3. A horizontal line is drawn at the infinite-acting radial flow line using late-time pressure derivative points.
4. The coordinates of the point A (t_i and ΔP_i) from fig. 2.1, where the unit-slope line and the infinite-acting horizontal line intersect is read thus $\Delta P_i = (t\times\Delta P')_i = (t\times\Delta P')_r$ in all steps.
5. Coordinates of the peak point (t_x and $(t\times\Delta P')_x$) on the pressure derivative curve is read.
6. A convenient time t_r and its corresponding ΔPr from the pressure curve during infinite-acting radial flow is read.
7. The permeability is calculated using Equation. 2.6.12.
8. The wellbore storage coefficient is also calculated from Equation 2.6.7 using t_i and ΔP_i or any convenient t and ΔP values on the unit slope line.
9. The skin factor is calculated from Equation 2.6.16.
10. The correctness and accuracy of the permeability, skin and wellbore storage is verified by calculating the time of intersection, t_i, of the unit-slope and infinite-acting straight lines using Equation 2.6.17. This step is necessary only if there is considerable noise in the pressure derivative value.
    a) If the calculated time is approximately equal to the time of intersection, t_i, observed in Fig. 2.1, it implies that the peak, the unit-slope and horizontal lines are in their correct position, and hence, the estimated skin, permeability and wellbore storage are correct.
    b) If the calculated and observed intersection times are vary significantly, a new peak is chosen and then Steps 4 through 9 repeated until the calculated and observed intersection times are the same.

2.7 Temperature disturbance in a Well

The formation temperature is determined by temperature disturbance caused by the circulating of the drilling mud. This measurement is done using electric logs. Edwardson et al (1962) investigated the use of numerical analysis to determine the temperature disturbances in the wellbore with respect to time. Differential equations were used in the paper to analyze the behavior of temperature of the formation during and after mud circulation. Plots of the temperature disturbance versus shut in

time for the different circulating time were generated. The exact method of solving differential equation was used in calculating for the temperature at the different circulating period. The temperature distribution around the wellbore is given by;

$$\frac{\partial^2 T}{\partial r^2} + \frac{1}{r}\frac{\partial T}{\partial r} = \frac{C_p \rho}{K}\frac{\partial T}{\partial t} \qquad (2.7.1)$$

It can also be expressed in dimensionless terms which is given by;

$$\frac{\partial^2 T}{\partial r^2{}_D} + \frac{1}{r_D}\frac{\partial T}{\partial r_D} = \frac{\partial T}{\partial t_D} \qquad (2.7.2)$$

The equation used in estimating the temperature was derived with the following assumptions;

i. Heat flow is due to conductivity only.
ii. Vertical heat flow in the formation is zero.
iii. Cylindrical symmetry exist, with the borehole as the axis.
iv. The pressure of the mud cake was neglected.
v. The effect heat generated by the bit action is neglected.
vi. The formation is treated like a radially infinite.

2.8 Thermal Effect on gas wells

In the research conducted by Fan et al (1999) presented a solution of heat transfer between a gas inside a wellbore and the surrounding formation. The outcome showed curves of different shapes as a result of thermal effects. This was mainly used in buildup test since none of well test methods including type curve was able to predict the pressure trend. This did not exhibit the true behavior of the reservoir and hence can be misleading. The semi-analytical model constructed for mass, momentum and energy balance equation was used in analyzing the thermal effect. These data were used in running a simulation and the following conclusion were presented in the paper;

i. The results of the simulation from a semi-analytical wellbore or reservoir model helped in predicting the effects on wellbore on pressure transient data especially from buildup tests of gas wells.

ii. The after flow rates lasted much longer due to heat loss effect compared to when there was no heat loss which is due to the fact that gas volumes decreases as gas cooled inside the tubing,

iii. The model can be used to estimate the minimum time required to obtain data without distortion by wellbore effect when designing the pressure build up test of gas wells.

iv. The duration of a pressure transient is very important during heat loss effect. When the true middle time region cannot be identified correctly, the pressure data can be easily misinterpreted as reservoir or boundary behavior.

v. The wellbore and reservoir properties can cause the pressure data affected by heat loss to behave the same way as heterogeneous reservoir.

vi. The model helps in identifying the heat loss effect in the pressure data and the true middle time region in order to ensure the accuracy of interpretation of the pressure data.

CHAPTER THREE
DERIVATION OF RELEVANT EQUATIONS

3.1 Introduction

The derivation of an energy equation for a homogenous porous medium involves the use the first law of thermodynamics to develop energy equations for the solid and fluid parts separately. These equations are averaged over an elementary control volume to obtain the general form of the model. Special attention is given to the fact that the fluid flow in a porous media is not ideal and the fluid flow is not isothermal. The change in potential and kinetic energies of the fluid flow is assumed to be negligible (Anh et al, 2008).

3.2 Mathematical Model

For the solid part, assuming no internal heat generation per unit volume of the solid material, the energy conservation equation associated with flow in an elastic porous medium for one-dimensional radial cylindrical flow heat influx equation for an infinite acting formation is given by (Anh et al, 2008):

$$\frac{1}{r}\frac{\partial}{\partial r}\left(r\frac{\partial T}{\partial r}\right)=\frac{1}{\alpha}\frac{\partial T}{\partial t} \tag{3.1}$$

Where the thermal diffusivity,α, is given by;

$$\alpha=\frac{K}{\rho C_p} \tag{3.2}$$

Considering a thin cylindrical shell element of reservoir thickness, dr, with a unit length.

Assumptions

i. *Rock properties such porosity, ø and density are assumed to be constant.*
ii. *Changes in thermal conductivity and Specific heat capacity are negligible.*
iii. *The initial temperature, T_i, (t=0) throughout the formation is uniform and equal.*
iv. *The boundary temperature in r direction T_i, (t>0) at any time.*
v. *The reservoir is heated at a constant heat rate, q at T_i.*

Where

ρ is the density of the reservoir

C_p is specific heat capacity

K is thermal conductivity

ω is thermal diffusivity

q is the heat injection influx at this slice

r is the radius of reservoir

therefore

$$T = T_1 - \frac{q}{4\pi K} Ei\left(\frac{-\omega}{t}\right) \tag{3.3}$$

Where ω is given by;

$$\omega = \frac{r^2}{4\lambda\alpha} \tag{3.4a}$$

Substituting equation 3.2 into 3.4a yields;

$$\omega = \frac{r^2 \rho C_p}{4\lambda K} \tag{3.4b}$$

but

$$x = \frac{\omega}{t} \tag{3.5a}$$

Therefore equation 3.5a becomes;

$$x = \frac{r^2 \rho C_p}{4\lambda K t} \tag{3.5b}$$

Also equation 3.3 can be expressed as;

$$T = T_1 - \frac{q}{4\pi K} Ei(-x) \tag{3.6}$$

From equation 3.6 the symbol *Ei* is an exponential integral defined by

$$Ei(-x) = -\int_x^{\infty} \frac{e^{-u}}{u}\, du$$

Where

u is dummy variable of integration

x is Boltzmann transformation variable

The exponential can be expressed in a convenient form by a series expansion (Craft and Hawkins 1959):

$$Ei(-x) = ln(1.781x) + \sum_{n=1}^{\infty} \frac{(-x)^n}{n.n!} \quad (3.7a)$$

Therefore equation 3.6 becomes

$$T = T_1 + 0.1832\frac{q}{K}\left[log(1.781x) + 0.434\sum_{n=1}^{\infty} \frac{(-x)^n}{n.n!} + 0.869s\right] \quad (3.8a)$$

The number of terms required depends upon the magnitude of x and the desired accuracy. For values of x less than 0.01, the exponential integral is closely approximated by;

$$Ei(-x) = ln(1.781x\ )\ for\ x < 0.01 \quad (3.7b)$$

Therefore temperature of the reservoir becomes;

$$T = T_1 + 0.1832\frac{q}{K}log(1.781x + 0.869s) \quad (3.8b)$$

Therefore assuming thermal skin, s is negligible

$$T = T_1 + 0.1832\frac{q}{K}log(1.781x) \quad (3.9)$$

A semi-log plot of T versus time gives a slope, *m* where

$$m = \frac{0.1832q}{K} \quad (3.10a)$$

This also implies that;

$$K = \frac{0.1832q}{m} \quad (3.10b)$$

3.2.1 Derivation of any expression for permeability

With the slope, *m* an equation can be derived for the permeability, K. Assuming that the gas is ideal, the intrinsic property of the formation is given by the expression, W (Wang et al).

$$W = \frac{1}{k} + C_A X \quad (3.11a)$$

$$W = \frac{\Delta PA}{2RT\mu Mh} \quad (3.11b)$$

But X can be expressed as;

$$X = \frac{M}{\mu A} \quad (3.12a)$$

And M can also be expressed as;

$$M = \rho A V_a \quad (3.12b)$$

Therefore equation 3.12a becomes;

$$X = \frac{V_a \rho}{\mu} \quad (3.12c)$$

Where

k is the permeability (m^2)

ΔP is the pressure drop (Pa)

A is cross-sectional area (m^2)

T is the sample temperature (K)

R is gas constant ($Jkg^{-1}K^{-1}$)

μ is gas viscosity (Pa s)

ρ is density of sample (Kgm^{-3})

V_a is the axial velocity of the sample (ms^{-1})

M is the mass flow rate (Kgs^{-1})

Also the thermal conductivity is given by;

$$K = \frac{\Delta Q h}{A \Delta t \Delta T} \quad (3.13a)$$

Therefore the cross-sectional area becomes;

$$A = \frac{\Delta Q h}{K \Delta t \Delta T} \quad (3.13b)$$

Substituting equation 3.13b into 3.11

$$W = \frac{\Delta P \Delta Q}{2RT\mu MK\Delta t\Delta T} \quad (3.14a)$$

But quantity of heat, ΔQ is given by

$$\Delta Q = MC_p\Delta T \quad (3.15)$$

Therefore substituting equation 3.15 into equation 3.14a gives

$$W = \frac{\Delta P C_p}{2RT\mu K\Delta t} \qquad (3.14b)$$

Equating equation 3.14b and 3.10

$$\frac{1}{k} + \mathrm{C_A}X = \frac{\Delta P C_p}{2RT\mu K\Delta t} \qquad (3.15a)$$

$$\frac{1}{k} = \frac{\Delta P C_p}{2RT\mu K\Delta t} - C_A X \qquad (3.15b)$$

Substituting equation 3.12a into 3.15b gives

$$\frac{1}{k} = \frac{\Delta P C_p}{2RT\mu K\Delta t} - C_A \frac{V_a \rho}{\mu} \qquad (3.15c)$$

Where

C_p is the specific heat capacity ($JKg^{-1}K^{-1}$)

h is the thickness of the formation (m)

ΔT is the temperature drop (K)

The inverse of equation 3.16c gives the permeability in m^2. It can however be converted to milli-darcy by dividing by the factor 9.869233E-13

3.2.2 Derivation of any expression for skin

Solving for skin

$$T = T_1 + 0.1832\frac{q}{K}\left[log(1.781x) + 0.434\sum_{n=1}^{\infty}\frac{(-x)^n}{n.n!} + 0.869s\right] \qquad (3.9a)$$

But

$$\left[0.434\sum_{n=1}^{\infty}\frac{(-x)^n}{n.n!}\right] \approx 0$$

Therefore equation 3.9a becomes;

$$T = T_1 + 0.1832\frac{q}{K}[log(1.781x) + 0.869s] \qquad (3.16)$$

Equation 3.16 can also be expressed as;

$$T = T_1 + m[log(1.781x) + 0.869s] \quad (3.17a)$$

$$T - T_1 = m[log(1.781x) + 0.869s] \quad (3.17b)$$

Making the skin the subject of equation 3.17b

$$s = \frac{1}{0.869}\left[\frac{T - T_1}{m} - log(1.781x)\right] \quad (3.18a)$$

Therefore skin is given by;

$$s = 1.151\left[\frac{T - T_1}{m} - log(1.781x)\right] \quad (3.18b)$$

3.3 Applying TDS technique to thermal transient

$$T = T_1 - \frac{q}{4\pi K} ln(1.781x) \quad (3.3)$$

where

$$x = \frac{r^2 \rho C_p}{4\lambda K t} \quad (3.5b)$$

Therefore equation 3.3 becomes;

$$T = T_1 - \frac{q}{4\pi K} ln\left(1.781 \frac{r^2 \rho C_p}{4\lambda K t}\right) \quad (3.19a)$$

Therefore temperature drop is given by;

$$T - T_1 = -\frac{q}{4\pi K} ln\left(1.781 \frac{r^2 \rho C_p}{4\lambda K t}\right) \quad (3.19b)$$

Equation 3.19b therefore becomes;

$$\Delta T = -\frac{0.1832q}{K} log\left(1.781 \frac{r^2 \rho C_p}{4\lambda K t}\right) \quad (3.19c)$$

Substituting slope, m into the equation 3.19c results to;

$$\Delta T = -m\, log\left(1.781 \frac{r^2 \rho C_p}{4\lambda K t}\right) \quad (3.19d)$$

Equation 3.19d can also be expressed as;

$$\Delta T = m\ log\left(\frac{4\lambda K t}{1.781 r^2 \rho C_p}\right) \tag{3.19e}$$

Re-arranging the terms results to;

$$\Delta T = m\ log\left(\frac{2.246\lambda K t}{r^2 \rho C_p}\right) \tag{3.20a}$$

Converting logarithm to the base ten to natural logarithm results to;

$$\Delta T = \frac{m}{2.303}\ ln\left(\frac{2.246\lambda K t}{r^2 \rho C_p}\right) \tag{3.20b}$$

Differentiating each side with respect to t

$$\Delta T' = \frac{m}{2.303}\left[\frac{\left(\frac{2.246\lambda K}{r^2 \rho C_p}\right)}{\left(\frac{2.246\lambda K t}{r^2 \rho C_p}\right)}\right] \tag{3.21}$$

Therefore equation 3.21 also results to;

$$\Delta T' = \frac{m}{2.303 t} \tag{3.22a}$$

This implies that;

$$\mathrm{t} \times \Delta T' = \frac{m}{2.303} \tag{3.22b}$$

And also the slope, m can also be expressed as;

$$(\mathrm{t} \times \Delta T') \times 2.303 = m \tag{3.22c}$$

Therefore the equation for thermal conductivity becomes

$$K = \frac{0.1832 q}{(\mathrm{t} \times \Delta T') \times 2.303} \tag{3.23}$$

Equation 3.22c can be substituted into equation 3.19b to obtain an equation for calculating skin.

$$s = 1.151\left[\frac{T - T_1}{(\mathrm{t} \times \Delta T') \times 2.303} - log(1.781x)\right] \quad (3.24)$$

3.4 Equations extended to real gases.

Some gases are not ideal gas and therefore do not exhibit properties that can be explained entirely using the ideal gas law. Some of these properties are compressibility factors, van der Waals forces, variable specific heat capacity, non-equilibrium effects, problems with molecular dissociation and the elementary reaction with variable composition.

The real gas equation is given by;

$$PV = znRT \quad (3.25)$$

$$z = \frac{PV}{nRT} \quad (3.26a)$$

Z is the compressibility factor (Z) which is measure of the deviation of the thermodynamic properties of a real gas from what is expected of ideal gases. The value of Z of ideal gases is always 1. This is not so for real gases but deviates positively or negatively, depending on the effect of the intermolecular forces of the gas. The closer a real gas is to its critical point or to its saturation point, the larger are the deviations of the gas from ideal behavior.

Z can also be expressed as the ratio of the actual volume of a real gas to the volume predicted by the ideal gas at the same temperature and pressure as the actual volume.

$$z = \frac{V_{actual}}{V_{ideal}} \quad (3.26b)$$

The number of moles of a substance, n can be expressed as;

$$n = \frac{m}{M} \quad (3.27a)$$

And the mass of a substance can be expressed as;

$$m = \rho V \quad (3.27b)$$

Therefore equation 3.27a becomes;

$$n = \frac{\rho V}{M} \tag{3.27c}$$

Substituting equation 3.27c into equation 3.26a gives;

$$z = \frac{PM}{\rho RT} \tag{3.26c}$$

The density of the gas can be estimated with the help of z. Pseudo reduced temperature and pseudo reduced pressure can help estimate z from charts.

$$\rho = \frac{PM}{zRT} \tag{3.28}$$

$$Reduced\ temperature, T_r = \frac{T}{T_c} \tag{3.29a}$$

$$Psuedo\ reduced\ Temperature, T_{pr} = \frac{T}{T_{pc}} \tag{3.29b}$$

$$Reduced\ pressure, P_r = \frac{P}{P_c} \tag{3.30a}$$

$$Psuedo\ reduced\ Pressure, P_{pr} = \frac{P}{P_{pc}} \tag{3.30b}$$

Where

T_c is the critical temperature

T_{pc} is the critical temperature

P_c is the critical pressure

P_{pc} is the critical pressure

With the help of P_{pr} and T_{pr} , the compressibility factor, z, can be estimated from charts.

3.4.1 Considering the Van Der Waals forces

The Van Der Waals equation is given by;

$$\left(P + \frac{a}{V^2}\right)(V - b) = RT \tag{3.31a}$$

Therefore making the pressure the subject of the equation results to;

$$P = \frac{RT}{(V - b)} - \frac{a}{V^2} \tag{3.31b}$$

Substituting equation 3.31b into equation 3.28 gives;

$$\rho = \frac{M}{zRT}\left(\frac{RT}{(V-b)} - \frac{a}{V^2}\right) \tag{3.32a}$$

$$\rho = \frac{M}{z(V-b)} - \frac{Ma}{zRTV^2} \tag{3.32b}$$

Where

$$a = \frac{27R^2T_c^2}{64P_c} \tag{3.33a}$$

and

$$a = \frac{RT_c}{8P_c} \tag{3.33b}$$

a and b are not true constants since they are different for different gases but its constant for the gas under investigation.

Where

P is the pressure

V is the volume

R is the real gas constant

T is temperature

a is the constant that accounts for the measure of the strength of the attraction between the gas molecules

b is the constant that account for the occupied by gas molecules, which decreases the available open volume

3.4.2 Pseudo Reduced Temperature function

$$T = T_1 + 0.1832\frac{q}{K}log(1.781x) \tag{3.9}$$

$$T_{pr} \times T_{pc} = \left(T_{pr_1} \times T_{pc}\right) + 0.1832\frac{q}{K}log(1.781x) \tag{3.34}$$

T_{pc} is constant for different types of natural gases. It can therefore be estimated from correlations. For the purpose of this work, Sutton's correlation for the determination of Pseudo-critical Properties of hydrocarbons when gas components are unknown.

$$T_{pc} = 169.2 + 349.5\gamma_h - 74.0\gamma_h^2 \tag{3.35}$$

Where

$\gamma_h$is the specific gas gravity of the hydrocarbon component (air=1.0) which range between 0.57 and 1.68. In this case, the gas under investigation is dry gas (thus no condensate is formed), and if the separator gas gravity is used, then $\gamma_h = \gamma_g$.

3.5 Developing type curves from dimensionless temperature and time functions for different r_D

The dimensionless temperature drop is a function of the dimensionless radius and dimensionless time. It is given by the expression (Edwardson et al, 1961);

$$\Delta T(r_D, t_D) = \frac{q}{2\pi Kh} P(r_D, t_D) \tag{3.36a}$$

But

$$P(r_D, t_D) = -\frac{1}{2} Ei\left(-\frac{r_D^2}{4t_D}\right) \tag{3.37a}$$

From equation 3.6 the symbol *Ei* is an exponential integral defined by

$$Ei(-x) = -\int_x^{\infty} \frac{e^{-u}}{u}\, du$$

Where

u is dummy variable of integration

x is Boltzmann transformation variable

$$X = \frac{r_D^2}{4t_D}$$

$$-Ei\left(-\frac{r_D^2}{4t_D}\right) \cong ln\left(-\frac{r_D^2}{4t_D}\right) - 0.5772 \tag{3.38a}$$

Equation 3.38a is also the same as;

$$-Ei\left(-\frac{r_D^2}{4t_D}\right) \cong ln\left(\frac{t_D}{r_D^2}\right) + 0.80907 \qquad (3.38b)$$

Therefore substituting equation 3.38b into eqaution3.37a yields;

$$P(r_D, t_D) = \frac{1}{2}\left[ln\left(\frac{t_D}{r_D^2}\right) + 0.80907\right] \qquad (3.37b)$$

Substituting equation 3.37b into eqaution3.36a yields;

$$\Delta T(r_D, t_D) = \frac{q}{4\pi Kh}\left[ln\left(\frac{t_D}{r_D^2}\right) + 0.80907\right] \qquad (3.36b)$$

Therefore the dimensionless temperature drop is given by;

$$\Delta T(r_D, t_D) = 0.1832\frac{q}{Kh}\left[log\left(\frac{t_D}{r_D^2}\right) + 0.80907\right] \qquad (3.36c)$$

Also, the dimensionless time is given by;

$$t_D = \frac{Kt}{\rho c_p r_w^2} \qquad (3.39)$$

Likewise the dimensionless radius is given by;

$$r_D = \frac{r}{r_w} \qquad (3.40)$$

Where

$T(r_D, t_D)$ is the dimensionless temperature, T_D

$P(r_D, t_D)$ is the dimensionless pressure, P_D

Therefore equation 3.16c becomes;

$$\Delta T_D = \frac{q}{4\pi Kh} ln\left(\frac{t_D}{r_D^2}\right) + 0.80907 \qquad (3.36d)$$

Now taking the derivative of equation 3.36d, gives a results of;

$$\Delta T'_D = \frac{q}{4\pi Kh}\left(\frac{1}{t_D r_D^2}\right) \quad (3.41a)$$

This implies that the derivative of the dimensionless temperature drop is given by;

$$\Delta T'_D = 0.07958\frac{q}{Kh}\left(\frac{1}{t_D r_D^2}\right) \quad (3.41b)$$

Re-arranging equation 3.41 gives;

$$t_D \times \Delta T'_D = 0.07958\frac{q}{Kh}\left(\frac{1}{r_D^2}\right) \quad (3.42)$$

A log log plot $t_D \times \Delta T'_D$ versus t_D is constructed with different dimension radius. As verification, equation 3.43 was used to compute for the temperature derivative and was found to give the same value as using equation 3.42. The results are shown the excel (TYPE CURVES FOR VARING r_D).

$$t_D \times \Delta T'_D = \frac{ln(t_{Di}/t_{Di-1})\Delta T_{Di+1}}{ln(t_{Di+1}/t_{Di})ln(t_{Di+1}/t_{Di-1})} + \frac{ln(t_{Di+1}t^2{}_{Di})\Delta T_{Di}}{ln(t_{Di+1}/t_{Di})ln(t_{Di}/t_{Di-1})} - \frac{ln(t_{Di+1}/t_{Di})\Delta T_{Di-1}}{ln(t_{Di}/t_{Di-1})ln(t_{Di+1}/t_{Di-1})}$$

(3.43)

3.6 Developing type curves from dimensionless temperature and time functions for different skin factors

The expression of dimensionless temperature in terms of skin factor is derived using equation 3.16. This is an expression for the temperature of the reservoir. In this case the skin factor is not assumed to be negligible.

$$T = T_1 + 0.1832\frac{q}{K}[log(1.781x) + 0.869s] \quad (3.16)$$

Making q/k is the subject of the equation yields;

$$\frac{q}{K} = \frac{\Delta T}{0.1832[log(1.781x) + 0.869s]} \quad (3.43)$$

Substituting equation 3.43 into equation into equation 3.42 yields;

$$t_D \times \Delta T'_D = 0.07958\frac{1}{h}\left(\frac{1}{r_D^2}\right)\left[\frac{\Delta T}{0.1832[log(1.781x) + 0.869s]}\right] \quad 3.44a)$$

Re-arranging the terms in equation 3.44 results to;

$$t_D \times \Delta T'_D = 2.302 \frac{1}{h}\left(\frac{1}{r_D^2}\right)\left[\frac{\Delta T}{[log(1.781x) + 0.869s]}\right] \qquad (3.44b)$$

Assuming r_D=1, then equation 3.60 becomes;

$$t_D \times \Delta T'_D = 2.302 \frac{1}{h}\left[\frac{\Delta T}{[log(1.781x) + 0.869s]}\right] \qquad (3.44c)$$

A log log plot $t_D \times \Delta T'_D$versus t_D is constructed with different skin factors. The results are shown the excel (TYPE CURVES FOR VARING SKIN)

CHAPTER FOUR

APPLICATION OF EQUATIONS TO FIELD DATA

4.1 Introduction

The equations derived in the previous chapter were tested with field data of known reservoir parameters. The idea of using data is to confirm and also act as a checked to validate these formulae and equation in chapter three. The reservoir data is shown in Table 4.1.

Table 4.1 Reservoir field data

Parameter	Value	Units
Thermal Conductivity, K	4.468292683	J/hrmK
Real gas Constant, R	8.314	J/K/mol
Pressure drop, ΔP	6.21E+07	Pa
Molar mass, M	5.5555E-09	pa hr
Density, ρ	0.668	kg/m3
Heat flux, q	1500	J/m2K
Shape factor, C_a	31.62	
Temperature, Ti	297.0389	K
Temperature drop, ΔT	306.15	K
Heat Capacity, C_p	1658	J/kg/K
Velocity of sample, V_a	0.03	m/hr
Wellbore radius, R_w	0.2033016	M
Time in 1 day, λ	24	Hr
Change in time, Δt	1.296	Hr
Permeability, k	10	mD
Skin factor, s	10	
Specific gravity, γ_g	0.64	
Reservoir pressure gradient	13572.33	Pa/m
Well depth	4572	m

The units of the data used in all calculation were in S. I. units. The pressure of the reservoir used was estimated using the reservoir pressure gradient and the well depth.

$$Reservoir\ Pressure = \frac{0.6psi}{ft} \times 15000ft$$

$$Reservoir\ Pressure = 9000psi = 62052820\ pa$$

Table 4.2 Temperature data for conventional thermal transient

Δt/days	ΔT/C	Δt/hr	ΔT/K	T/K
0.0245	10.5	0.588	283.65	295.65
0.0278	12.5	0.6672	285.65	297.65
0.0315	14.5	0.756	287.65	299.65
0.035	16.5	0.84	289.65	301.65
0.038	17	0.912	290.15	302.15
0.042	17.8	1.008	290.95	302.95
0.045	18.2	1.08	291.35	303.35
0.048	19	1.152	292.15	304.15
0.0515	19.1	1.236	292.25	304.25
0.054	21	1.296	294.15	306.15
0.058	22	1.392	295.15	307.15
0.063	23	1.512	296.15	308.15
0.067	24	1.608	297.15	309.15
0.07	24.5	1.68	297.65	309.65
0.072	25	1.728	298.15	310.15
0.074	26	1.776	299.15	311.15
0.076	27	1.824	300.15	312.15
0.078	28	1.872	301.15	313.15
0.08	28.5	1.92	301.65	313.65
0.0825	29	1.98	302.15	314.15
0.085	29.2	2.04	302.35	314.35
0.0875	29.5	2.1	302.65	314.65
0.09	30	2.16	303.15	315.15
0.092	30.4	2.208	303.55	315.55
0.094	30.8	2.256	303.95	315.95
0.096	31.2	2.304	304.35	316.35
0.098	31.6	2.352	304.75	316.75
0.1	32	2.4	305.15	317.15
0.11	33	2.64	306.15	318.15
0.12	35	2.88	308.15	320.15
0.13	37	3.12	310.15	322.15
0.14	39	3.36	312.15	324.15
0.15	40	3.6	313.15	325.15
0.16	41	3.84	314.15	326.15
0.17	43	4.08	316.15	328.15
0.18	45	4.32	318.15	330.15
0.19	47	4.56	320.15	332.15
0.2	49	4.8	322.15	334.15
0.22	51	5.28	324.15	336.15
0.24	53	5.76	326.15	338.15
0.26	55	6.24	328.15	340.15
0.28	57	6.72	330.15	342.15
0.3	59	7.2	332.15	344.15
0.32	61	7.68	334.15	346.15
0.34	63	8.16	336.15	348.15
0.36	65	8.64	338.15	350.15

0.38	67	9.12	340.15	352.15
0.4	69	9.6	342.15	354.15
0.42	70	10.08	343.15	355.15
0.44	71	10.56	344.15	356.15
0.46	72	11.04	345.15	357.15
0.48	73	11.52	346.15	358.15
0.5	74	12	347.15	359.15
0.52	75	12.48	348.15	360.15
0.54	76	12.96	349.15	361.15
0.56	77	13.44	350.15	362.15
0.58	78	13.92	351.15	363.15
0.59	79	14.16	352.15	364.15
0.6	80	14.4	353.15	365.15
0.62	81	14.88	354.15	366.15
0.64	82	15.36	355.15	367.15
0.66	83	15.84	356.15	368.15
0.68	84	16.32	357.15	369.15
0.7	85	16.8	358.15	370.15
0.725	86	17.4	359.15	371.15
0.75	87	18	360.15	372.15
0.775	88	18.6	361.15	373.15
0.8	89	19.2	362.15	374.15
0.83	90	19.92	363.15	375.15
0.87	91	20.88	364.15	376.15
0.9	92	21.6	365.15	377.15
0.93	93	22.32	366.15	378.15
0.97	94	23.28	367.15	379.15
1	95	24	368.15	380.15
1.1	97	26.4	370.15	382.15
1.2	99	28.8	372.15	384.15
1.3	101	31.2	374.15	386.15
1.4	103	33.6	376.15	388.15
1.5	105	36	378.15	390.15

A plot of ΔT versus shut in time in hours on a semi log plot is used to estimate the slope, m which inturn will help estimate the thermal conductivity, k.

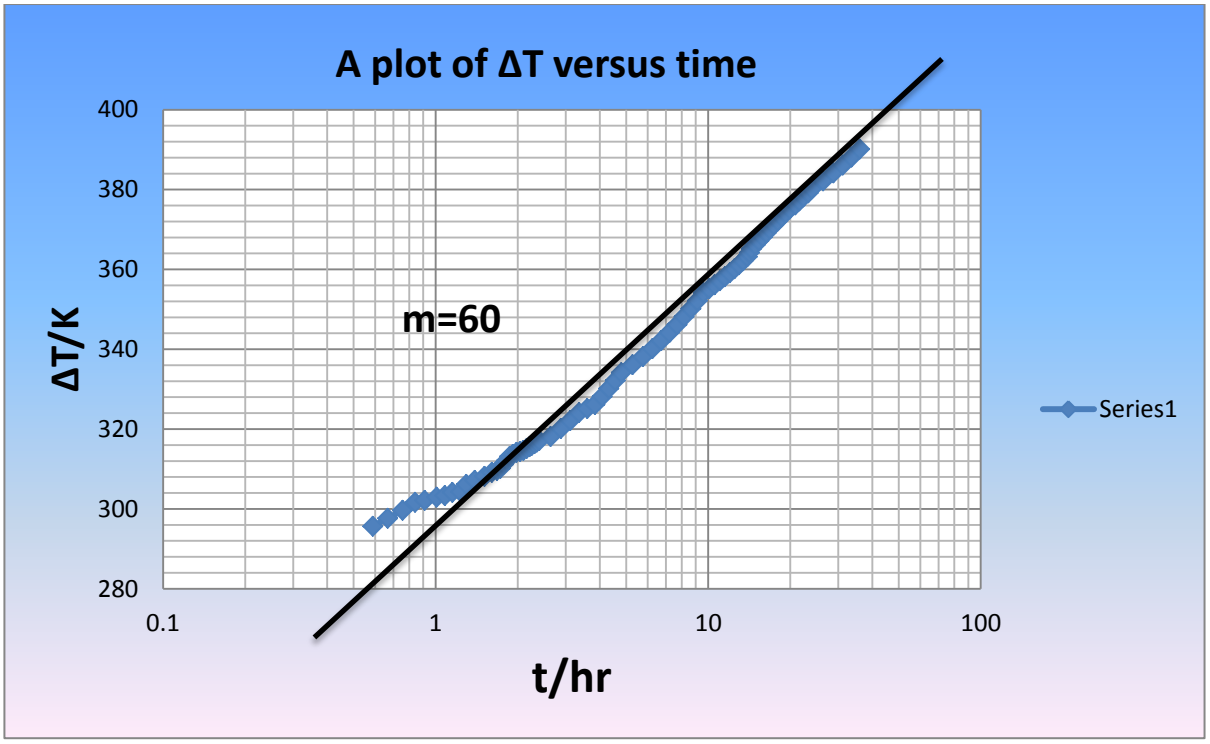

Fig 4.1 A graph of temperature drop versus shut in time

4.1.1 Estimating the Permeability using Semi-log thermal transient

$$Thermal\ conductivity, K = \frac{0.1832q}{m} = \frac{0.1832(1500)}{60} = 4.58$$

Therefore the permeability can be estimated from equation 3.16c

$$\frac{1}{k} = \frac{\Delta P C_p}{2RT\mu K \Delta t} - C_A \frac{V_a \rho}{\mu}$$

$$\frac{1}{k} = \frac{62052820(1658)}{2(8.314)(297.0389)(5.555E-09)(4.58)(1.296)} - 31.62\frac{(0.03)(0.668)}{5.555E-09}$$

$$\frac{1}{k} = 1E+14$$

$$k = 9.7E-15\ m^2$$

$$k = 9.7E-15 \div 9.869233E-15$$

$$k = 0.00984\ D$$

$$k = 9.84\ mD$$

4.1.2 Estimating the skin using Semi-log thermal transient

Also the skin can be estimated from the using equation 3.19b

$$s = 1.151\left[\frac{T - T_1}{m} - log(1.781x)\right] \ldots\ldots\ldots\ldots\ldots\ldots\ldots (3.19b)$$

$$x = \frac{r^2\rho C_p}{4\lambda K t} = \frac{(0.2033016^2)(0.668)(1658)}{4(24)(4.468292683)(1.296)} = 0.08234$$

At t=1.296hr, T is 386.15K and Ti is 295.65K

$$s = 1.151\left[\frac{386.15 - 295.65}{61.5} - log(1.781 \times 0.08234)\right]$$

$$s = 2.65335$$

4.2 Applying the TDS technique to the temperature data

The temperature data was applied to the equations derived using the TDS technique in chapter. The result of the temperature derivative is shown below.

Table 4.3 Temperature data for TDS thermal transient

Δt/hr	ΔT	t*ΔT'	3-smoothed point
0.588	10.5		
0.6672	12.5	15.92	0
0.756	14.5	17.62	0
0.84	16.5	11.74	0
0.912	17	6.94	9.88371157
1.008	17.8	6.69	7.700657332
1.08	18.2	9.21	10.48681153
1.152	19	7.15	12.88219474
1.236	19.1	24.52	13.87594195
1.296	21	29.68	14.31126918
1.392	22	13.11	14.22610634
1.512	23	14.47	15.60621322
1.608	24	13.42	14.94056211

1.68	24.5	15.27	20.87865021
1.728	25	27.25	28.61615885
1.776	26	37.00	25.14110706
1.824	27	38.00	25.43570436
1.872	28	29.00	25.53948666
1.92	28.5	18.17	21.7827971
1.98	29	11.40	18.91030377
2.04	29.2	8.55	14.21909135
2.1	29.5	14.10	14.13017834
2.16	30	18.00	14.2640056
2.208	30.4	18.40	16.54847827
2.256	30.8	18.80	17.85430986
2.304	31.2	19.20	23.37077338
2.352	31.6	19.60	20.64614562
2.4	32	18.17	20.34777246
2.64	33	17.02	27.90340816
2.88	35	24.03	23.444882
3.12	37	26.03	21.4708327
3.36	39	20.52	20.85670656
3.6	40	15.01	23.51372331
3.84	41	24.52	26.17153553
4.08	43	34.02	27.82710526
4.32	45	36.02	31.83085629
4.56	47	38.02	31.4763951
4.8	49	32.69	31.00177427
5.28	51	22.03	31.54468803
5.76	53	24.03	27.61966947
6.24	55	26.03	26.2997247
6.72	57	28.02	26.23350522
7.2	59	30.02	28.21646797
7.68	61	32.02	30.20176884
8.16	63	34.02	32.18895386
8.64	65	36.02	30.82822406
9.12	67	38.02	29.13739235
9.6	69	29.51	27.11591697
10.08	70	21.01	25.76526547
10.56	71	22.01	24.08284737
11.04	72	23.01	22.0684591
11.52	73	24.01	23.06545986
12	74	25.01	24.06271326
12.48	75	26.01	25.06018856
12.96	76	27.01	26.05785984
13.44	77	28.01	30.26970249
13.92	78	48.67	37.04553736
14.16	79	59.00	38.34393401

14.4	80	49.67	35.44243905
14.88	81	31.01	38.4410438
15.36	82	32.01	39.73973717
15.84	83	33.01	35.2608849
16.32	84	34.00	31.70879959
16.8	85	31.78	
17.4	86	29.01	
18	87	30.01	
18.6	88	31.01	
19.2	89	29.49	
19.92	90	24.57	
20.88	91	26.04	
21.6	92	30.01	
22.32	93	27.54	
23.28	94	29.02	
24	95	29.96	
26.4	97	22.03	
28.8	99	24.03	
31.2	101	26.03	
33.6	103	28.02	
36	105		

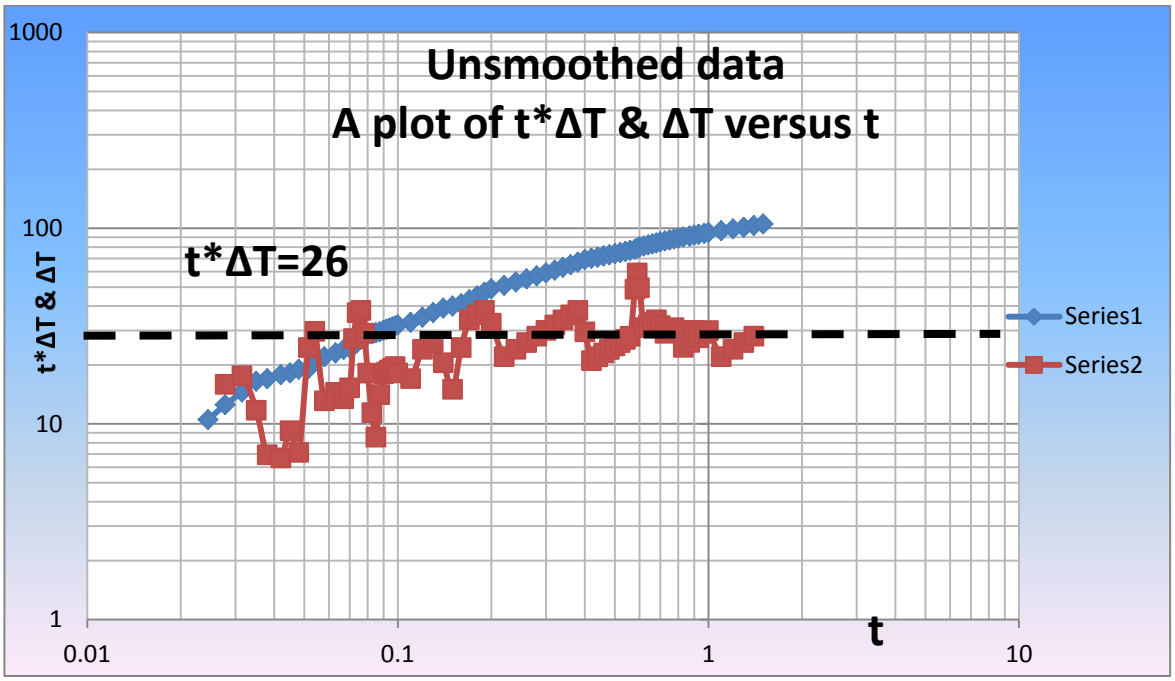

Fig 4.2 A graph of t*ΔT versus shut in time (unsmoothed)

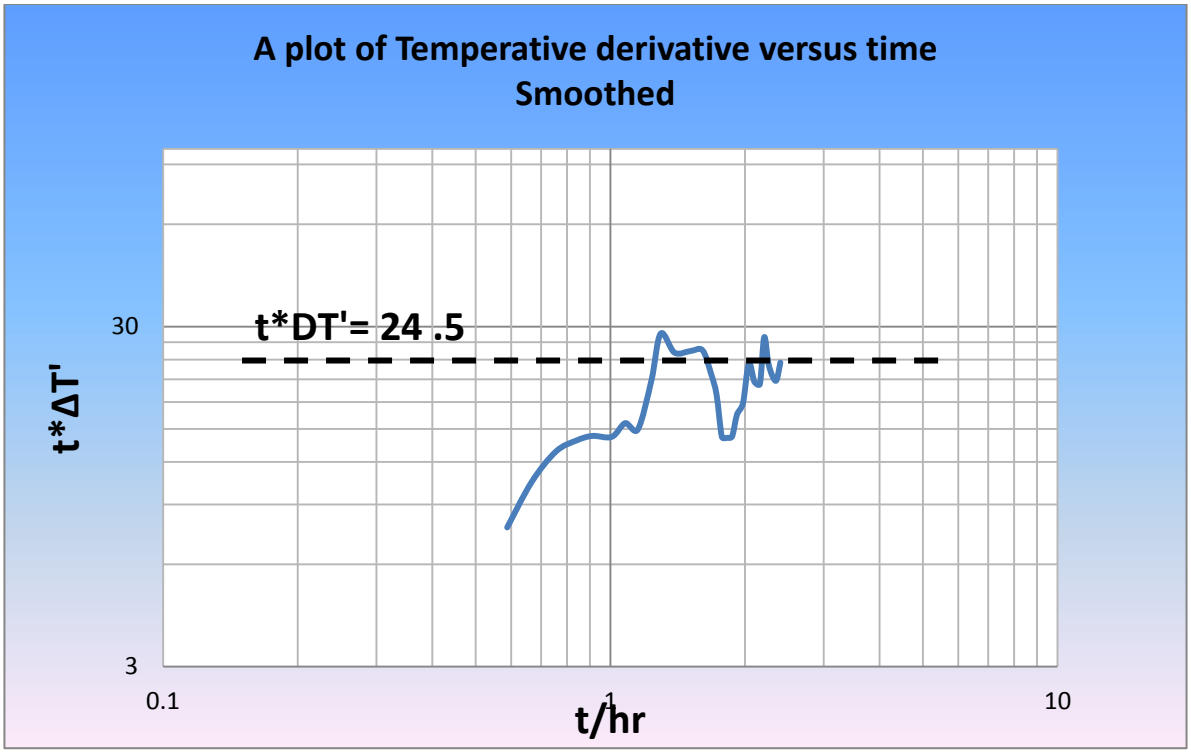

Fig 4.3 A graph of t*ΔT versus shut in time (smoothed)

4.2.1 Estimating the permeability using TDS thermal transient

From equation 3.1, thermal conductivity is given by;

$$K = \frac{0.1832q}{(\mathrm{t} \times \Delta T') \times 2.303}$$

$$K = \frac{0.1832 \times 1500}{(24.5) \times 2.303}$$

$$K = 4.87031$$

Therefore the permeability can be estimated from equation 3.16c

$$\frac{1}{k} = \frac{\Delta P C_p}{2RT\mu K \Delta t} - C_A \frac{V_a \rho}{\mu} \quad \ldots\ldots\ldots\ldots\ldots\ldots\ldots\ldots\ldots\ldots\ldots\ldots\ldots\ldots (3.16c)$$

$$\frac{1}{k} = \frac{\Delta P C_p}{2RT\mu K \Delta t} - C_A \frac{V_a \rho}{\mu}$$

$$\frac{1}{k} = \frac{62052820(1658)}{2(8.314)(297.0389)(5.555\text{E}-09)(4.87031)(1.296)} - 31.62\frac{(0.03)(0.668)}{5.5555\text{E}-09}$$

$$\frac{1}{k} = 9.68223E + 13$$

$$k = 1.03282E - 14m^2$$

$$k = 1.03282E - 14 \div 9.869233E - 13$$

$$k = 0.010465048D$$

$$k = 10.465048\, mD$$

4.2.2 Estimating the skin using TDS thermal transient

Also the skin can be estimated from equation 3.23

$$s = 1.151\left[\frac{T - T_1}{(\text{t} \times \Delta T') \times 2.303} - log(1.781x)\right]$$

$$x = \frac{r^2\rho C_p}{4\lambda Kt} = \frac{0.08128^2)(0.668)(1658)}{4(24)(6.3574)(1.296)} = 0.07555$$

At t=1.296hr, T is 386.15K and Ti is 295.65K

$$s = 1.151\left[\frac{386.15 - 295.65}{24.5 \times 2.303} - log(1.781 \times 0.07555)\right]$$

$$s = 2.8488$$

4.3 By applying this Pseudo Reduced Temperature function

From the reservoir, specific gravity of gas, $\gamma_g$is 0.64, therefore $P_{pc}$and T_{pc} were estimated using Sutton's correlation and a semi log plot of Tpr versus t was done.

$$T_{pc} = 169.2 + 349.5\gamma_h - 74.0\gamma_h^2 = 362.5696\, R$$

Table 4.3 Temperature data for pseudo temperature function

	S.G(gas)	0.64	
	Ppc	671.4854	Psi
	Tpc	362.5696	R
t/hr	T/K	T/R	Tpr
0.59	295.65	532.17	1.47
0.67	297.65	535.77	1.48
0.76	299.65	539.37	1.49
0.84	301.65	542.97	1.50
0.91	302.15	543.87	1.50
1.01	302.95	545.31	1.50
1.08	303.35	546.03	1.51
1.15	304.15	547.47	1.51
1.24	304.25	547.65	1.51
1.30	306.15	551.07	1.52
1.39	307.15	552.87	1.52
1.51	308.15	554.67	1.53
1.61	309.15	556.47	1.53
1.68	309.65	557.37	1.54
1.73	310.15	558.27	1.54
1.78	311.15	560.07	1.54
1.82	312.15	561.87	1.55
1.87	313.15	563.67	1.55
1.92	313.65	564.57	1.56
1.98	314.15	565.47	1.56
2.04	314.35	565.83	1.56
2.10	314.65	566.37	1.56
2.16	315.15	567.27	1.56
2.21	315.55	567.99	1.57
2.26	315.95	568.71	1.57
2.30	316.35	569.43	1.57
2.35	316.75	570.15	1.57
2.40	317.15	570.87	1.57
2.64	318.15	572.67	1.58
2.88	320.15	576.27	1.59
3.12	322.15	579.87	1.60
3.36	324.15	583.47	1.61
3.60	325.15	585.27	1.61
3.84	326.15	587.07	1.62
4.08	328.15	590.67	1.63
4.32	330.15	594.27	1.64
4.56	332.15	597.87	1.65

4.80	334.15	601.47	1.66
5.28	336.15	605.07	1.67
5.76	338.15	608.67	1.68
6.24	340.15	612.27	1.69
6.72	342.15	615.87	1.70
7.20	344.15	619.47	1.71
7.68	346.15	623.07	1.72
8.16	348.15	626.67	1.73
8.64	350.15	630.27	1.74
9.12	352.15	633.87	1.75
9.60	354.15	637.47	1.76
10.08	355.15	639.27	1.76
10.56	356.15	641.07	1.77
11.04	357.15	642.87	1.77
11.52	358.15	644.67	1.78
12.00	359.15	646.47	1.78
12.48	360.15	648.27	1.79
12.96	361.15	650.07	1.79
13.44	362.15	651.87	1.80
13.92	363.15	653.67	1.80
14.16	364.15	655.47	1.81
14.40	365.15	657.27	1.81
14.88	366.15	659.07	1.82
15.36	367.15	660.87	1.82
15.84	368.15	662.67	1.83
16.32	369.15	664.47	1.83
16.80	370.15	666.27	1.84
17.40	371.15	668.07	1.84
18.00	372.15	669.87	1.85
18.60	373.15	671.67	1.85
19.20	374.15	673.47	1.86
19.92	375.15	675.27	1.86
20.88	376.15	677.07	1.87
21.60	377.15	678.87	1.87
22.32	378.15	680.67	1.88
23.28	379.15	682.47	1.88
24.00	380.15	684.27	1.89
26.40	382.15	687.87	1.90
28.80	384.15	691.47	1.91
31.20	386.15	695.07	1.92
33.60	388.15	698.67	1.93
36.00	390.15	702.27	1.94

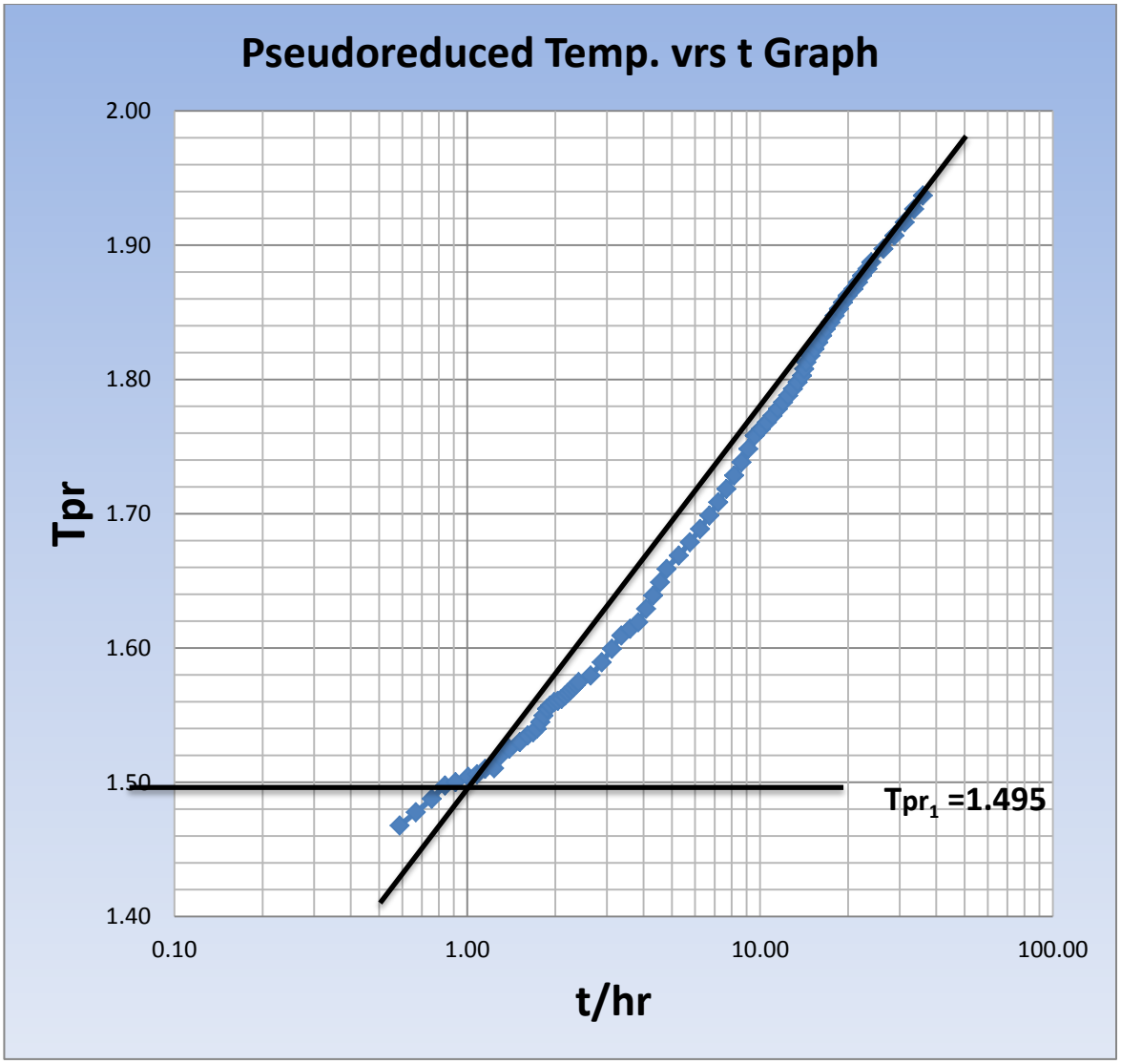

Fig. 4.4 A graph of pseudo reduced temperature drop versus shut in time

From the plot, T_{pr_1} was estimated to be 1.495. This is the y-intercept thus at time, t=1.

$$T_{pr} \times T_{pc} = \left(T_{pr_1} \times T_{pc}\right) + 0.1832 \frac{q}{K} log(1.781x) \tag{3.34}$$

$$T_{pr} \times T_{pc} = \left(T_{pr_1} \times T_{pc}\right) + 0.1832 \frac{q}{K} log(1)$$

$$T_{pr} \times T_{pc} = \left(T_{pr_1} \times T_{pc}\right)$$

This implies that;

$$T_{pr} = T_{pr_1}$$

Therefore, the initial reservoir temperature, T_1 can be also estimated from equation 3.34.

$$T_{pr} \times T_{pc} = \left(T_{pr_1} \times T_{pc}\right) + 0.1832 \frac{q}{K} log(1.781x) \quad (3.34)$$

But

$$T_1 = T_{pr_1} \times T_{pc}$$

$$T_1 = 1.495 \times 362.5696$$

$$T_1 = 542.04\ R$$

$$T_1 = 301.1333\ K$$

CHAPTER FIVE

DISCUSSION OF RESULTS

In the chapter four of this research work, reservoir data was applied to the equations on the normal thermal transient and the thermal transient using TDS technique for estimating reservoir parameters like permeability and skin. It was also applied to real pseudo-reduced temperature functions derived in chapter three to estimate initial reservoir temperature. Type curves for dimensionless temperature and its derivatives for different values of dimensionless radii as well as the dimensionless temperature derivative for different values of dimensionless skin factors were generated.

5.1 Discussion of results conventional thermal transient and thermal transient using TDS technique

The temperature data derived from reservoir at different shut-in times was plotted on a semi log plot. The graph gave some how a linear positive slope as shown in Fig.4.1.

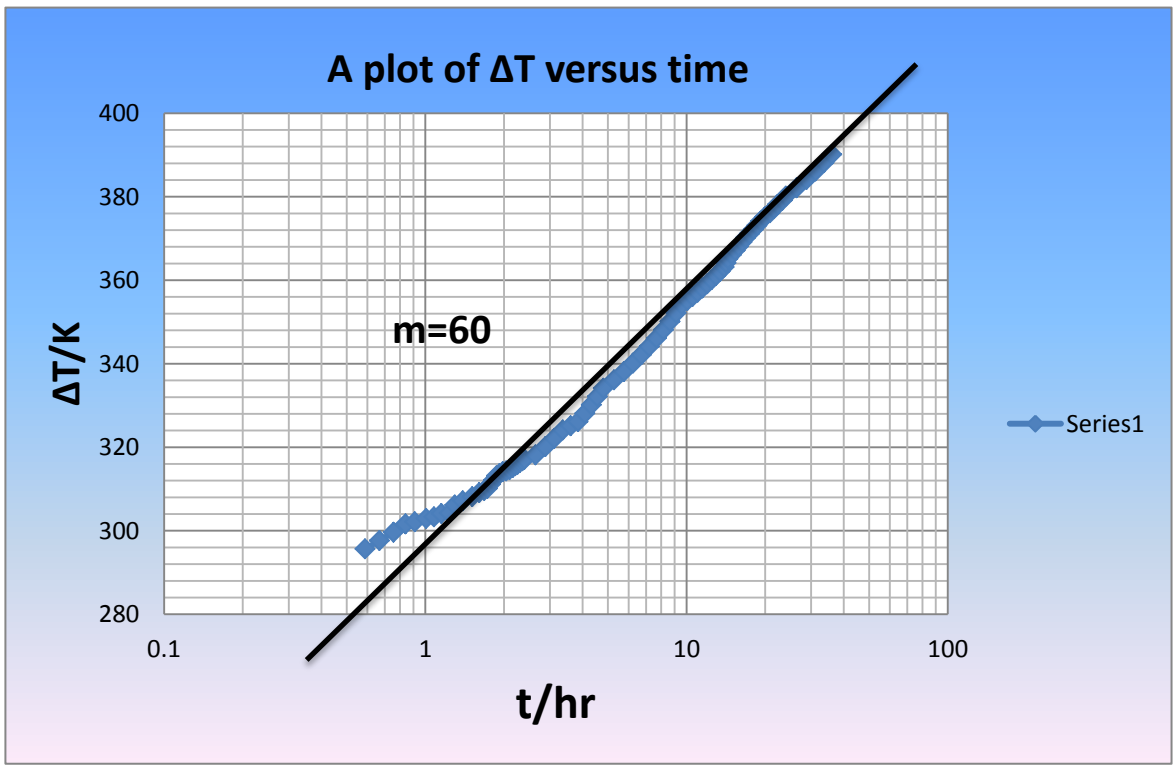

Fig. 4.1 A graph of temperature drop versus shut in time

The slope, m, was estimated to be 60. The slope was then used to estimate the thermal conductivity, k of the reservoir using equation 3.10b and gave a results of 4.58. The TDS technique was applied to the same temperature data. The TDS temperature derivative data versus time was plotted on a log log graph as shown in Fig. 4.3.

The infinite acting line portion of the curve was estimated to be 24.5 which gives approximately the same slope as that of the Fig. 5.2 using equation 3.22c. This slope was also used in estimating the thermal conductivity of 4.87. This values are approximately the same and therefore act as confirmation. The permeability of the reservoir was estimated using the thermal conductivities derived from the semi log thermal transient and thermal transient using TDS technique which were 9.84 mD and 10.47 mD respectively using equation 3.15c. These values approximately equal to the permeability of the reservoir derived from pressure transient test which is 10 mD. This therefore confirms that estimating permeability from semi log thermal transient and thermal transient using TDS technique is very reliable.

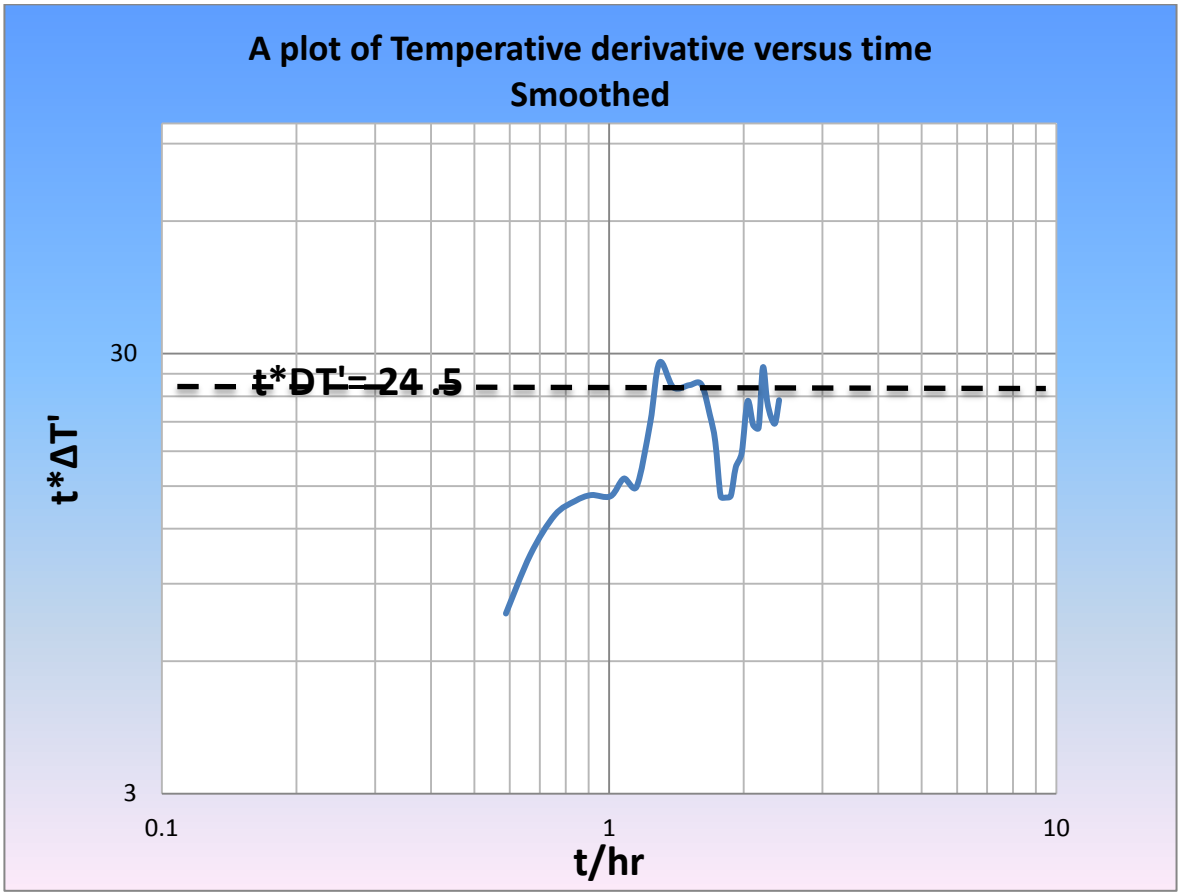

Fig. 4.3 A graph of t*ΔT versus shut in time (smoothed)

The skin factors were also estimated using eqaution 3.18b for the semi log thermal transient method and equation 3.24 for thermal transient using TDS technique. The semi log thermal transient gave 2.65. and the thermal transient using TDS gave 2.85 which is quite far from the skin factor of the reservoir which was 10. One can therefore conclude that these does not accurately estimate the skin factors of the reservoir.

Table 5.1 Comparison of Semi-log and TDS methods of thermal transient

Parameters	Semi-log Thermal transient	TDS Applied to thermal transient	True Value of Reservoir
Permeability (mD)	9.84	10.465	10
Skin	2.65355	2.8488	10

5.2 Benefits of thermal transient test to Pressure transient test.

From this research work, some the benefits of thermal transient test over pressure transient test are;

i. Thermal transient testing is less expensive to carry out. Pressure transient testing methods are expensive to conduct due to the requirements, planning, equipment and environmental regulations involved. Thermal transient testing tends to be less expensive since it doesn't involve much planning and special equipment when been conducted.

ii. The equipment used in recording temperature data in pressure transient test are bulky compared to thermal transient test where equipment such as thermocouple and fiber optic sensor are used.

iii. The permeability estimated from pressure transient test is very sensitive to the slope and hence any slight mistake made in the selection of the right region for the slope will result in wrong permeability values. In thermal transient testing, the reservoir permeability is affected by the properties of the fluid.

iv. The duration of pressure transient test is very essential in the determination of reservoir parameters whereas the duration of thermal transient test is not very important in the determination of reservoir parameters. It can be carried out at short time test. Unlike pressure transient testing, thermal transient testing is not significantly affected by short time test.

v. It gives better results when there is wellbore storage. Wellbore storage does not affect the permeability and skin factor estimated in thermal transient testing as they do pressure transient testing.

vi. Also, thermal transient is more ideal for certain recovery processes like steam injection and in situ combustion since the heat produced or injected can be used in the thermal transient test analysis.

5.3 Discussion of results of the real pseudo reduced temperature functions

This research work wa extended to gas reservoir using pseudo-reduced temperature functions. The pseudo-reduced temperature was estimated for each time step using sutton's correlation for pseudo critical temperature in equation 3.35b. The specific gravity used in estimating pseudo critical temperature was that of the reservoir which was 0.64. A plot of the pseudo reduced temperature versus time on a log log graph as shown in fig. 5.3. The graph gave some how linear slope which show that the rate of change of the pseudoreduced temperature is directed proportion to the change with time.

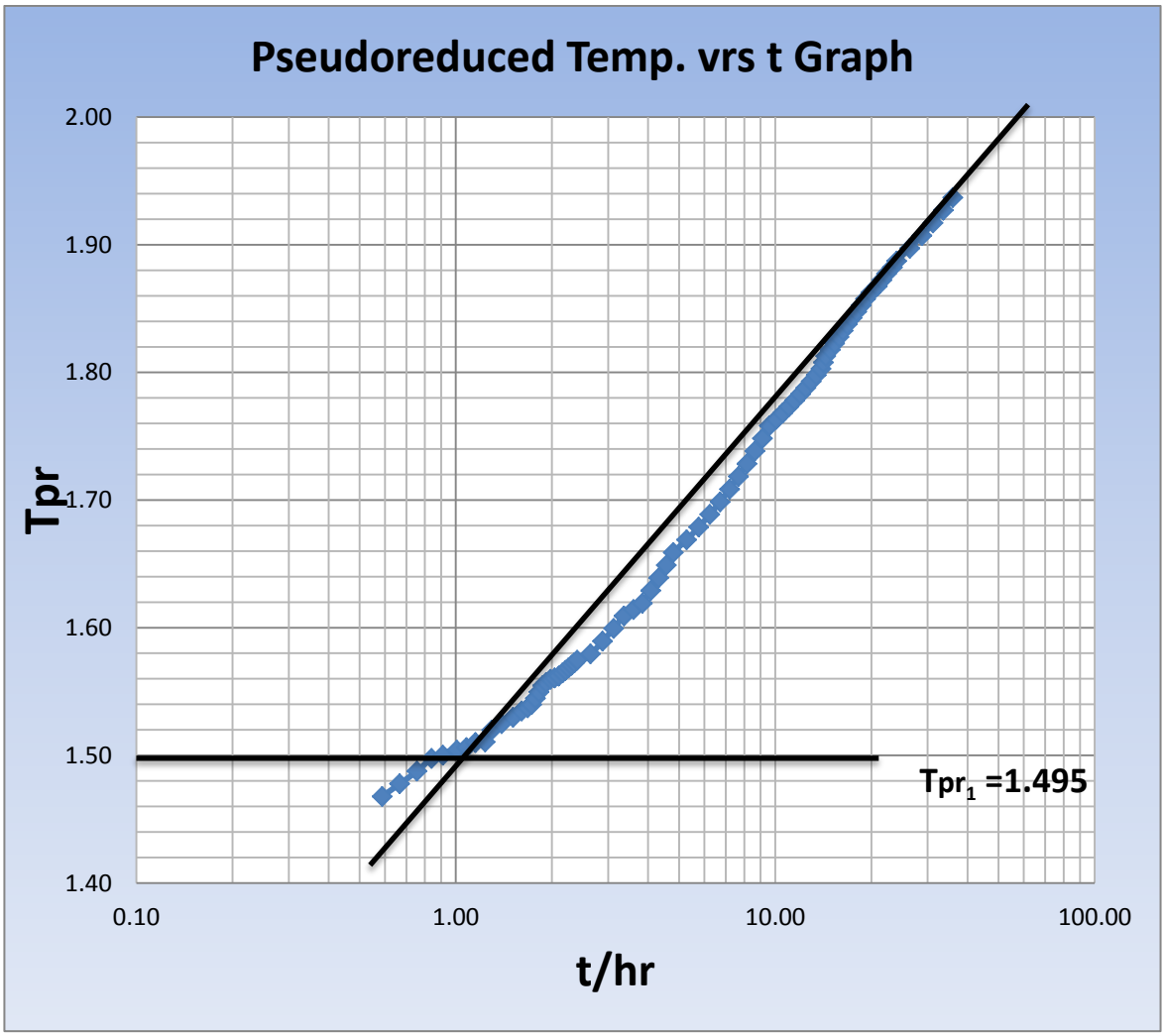

Fig. 4.4 A graph of pseudo reduced temperature drop versus shut in time

The initial pseudo reduced temperature can be estimated at y-axis intercept which can then be used to estimate the reservoir initial temperature, Ti. The initial

reservoir temperature computed was 301.13 K which almost the same as the original initial reservoir temperature which is 297.04. The difference of about 4 K is not quite significant; therefore the pseudo reduced temperature function can be used in estimating initial reservoir temperature.

Table 5.2 Comparison of conventional and TDS methods of thermal transient

Original Initial reservoir temperature(K)	Computed initial reservoir temperature(K)
297.04	301.13

5.4 Discussion of type curves generated for the dimensionless temperature derivative for different dimensionless radius.

The dimensionless temperature derivative data was computed using equation 3.42 and the results shown in appendix A. It was then plotted on a log log graph versus the dimensionless time. The graph was done for different dimensionless radius on the same graph sheet. It must be said that the dimensionless radius varied between 1.0 and 50 as shown in fig.5.4. The dimensionless temperature values started giving negative value at r_D= 1.3 and above. It must also be noted that dimensionless temperature values using equation 3.1 and 3.4 were the same and acting as a confirmation. The dimensionlesss tempearture derivative values computed were inversely proportion to the dimensionless radius values.

The dimensionless temperature curve exhibit the trend of a well with a wellbore storage and skin factor in an infinite reservoir with homogenous behaviour. It can be observed that the rate of change of temperature at each time step is constant which may be as a result of homogenous behavoir of the reservoir. This is as a result of temperature tranfer in fluid by thermal conductivity. At the different values of dimensionless radii, the curves had a constant slope of 4.25.

The dimensionless temperature derivative curve exhibit a trend of radial flow through the life of the well. It also correspond with a well with a vertical infinite conductivity fracture in an infinite reservoir with homogenous behaviour. At the different values of dimensionless radii, the curves had a constant slope of zero.

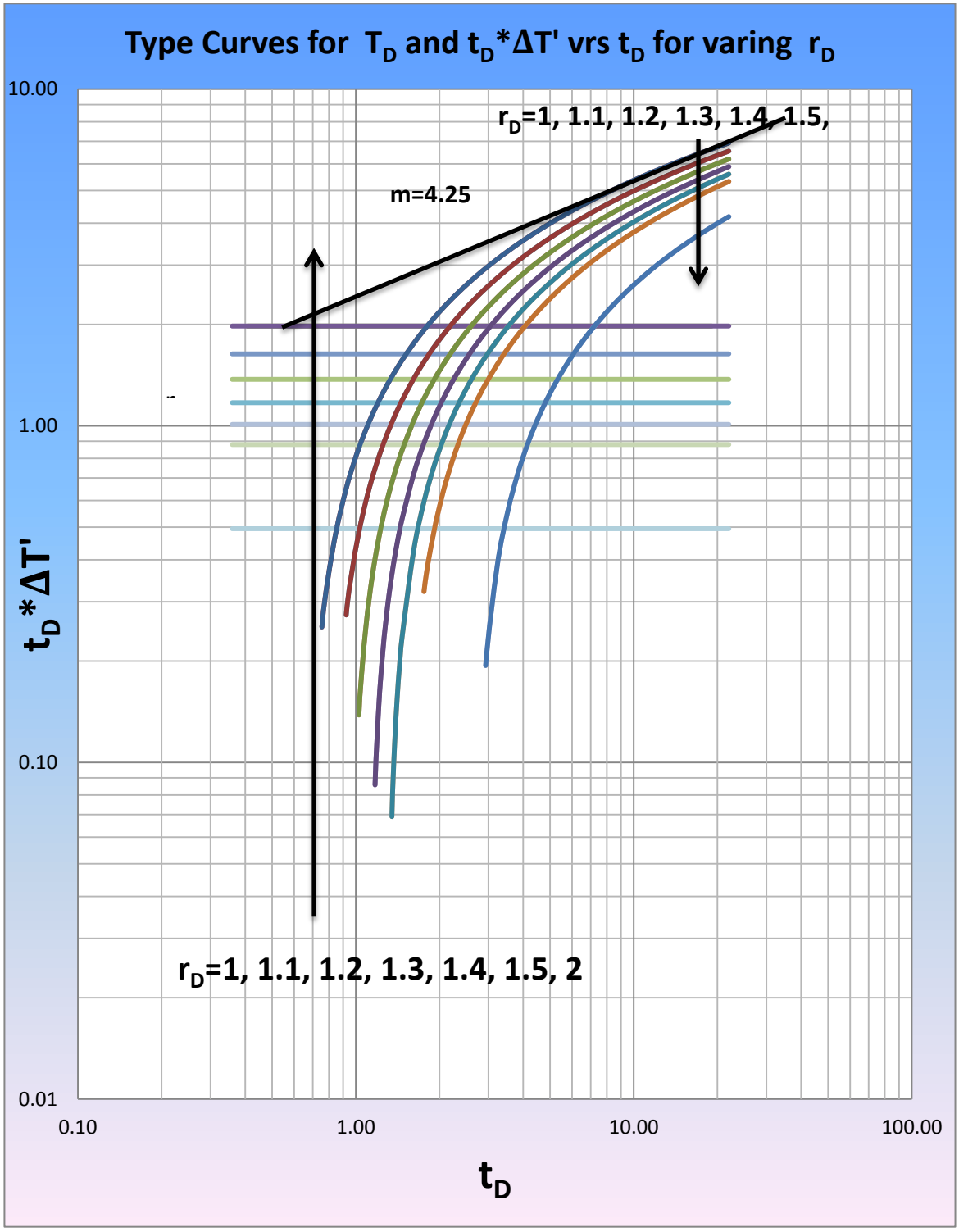

Fig. 5.1 Type curve of dimensionless temperature derivatives for varying dimensionless radius

5.5 Discussion of type curves generated for the dimensionless temperature derivative for different skin factors.

The dimensionless temperature derivative data was computed using equation3.44b derived in chapter three and the results shown in appenix B. A plot of dimensionless temperature derivative versus dimensionless time is constructed on a log log graph. This graph was done for different dimensionless skin factors on the same graph sheet. Skin factors were varies between -4 and 30 and then used in computing for the dimensionless teperature derivative values as shown in fig. 5.4. The values yielded negative values for skin factor values of zero(no damage or stimulation) and below (stimulation). The dimensionlesss tempearture derivative values computed were directly proportion to the skin factors.

The dimensionless temperature derivative curve for the part of the reservoir that was stimulated(thus $s<0$) exhibit downwards sloping trend which is an indication of a constant pressure boundary. The downwards sloping may be due to the fact that the there was temperature drop in the reservoir during its producing life.

The part of the well which was neither stimulated nor damaged(thus $s=0$) also exhibit downwards sloping trend although not as evident as when reservoir was stimulated. This confirms that the reservoir has a constant pressure boundary.

The dimensionless temperature derivative curve for the part of the reservoir that was damaged (thus $s>0$) exhibit a trend of a radial flow throughout the life of the well but slopes gently upwards indicating a semi-infinite behavoiur. This may be due to the activities that caused the formation damage which provide heat sources in the reservoir to compensate for drop in temperature during its producing life. Some of the formation damage mechanism that are likely to create heat sources are fluids and Polymers, drilling, running pipe and cementing, perforating, well completions, during production and workover (Schlumberger).

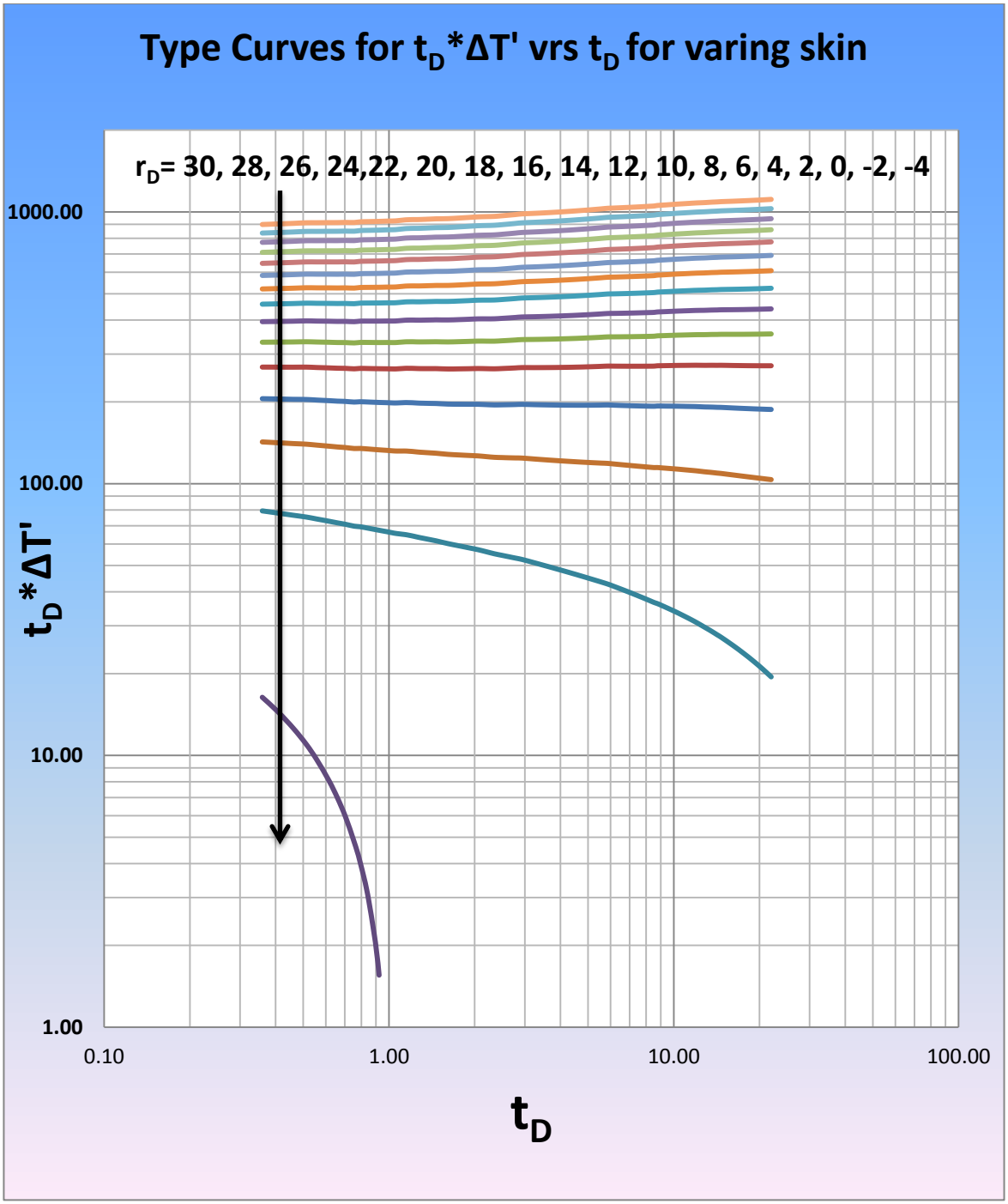

Fig. 5.2 Type curve of dimensionless temperature derivatives for varying skin factors

CHAPTER SIX
CONCLUSION AND RECOMMENDATIONS

6.1 Conclusion

From the analysis of the results obtained in this research work, the following conclusions can be made;

a. Thermal transient testing can be used as an alternative for the estimation of the permeability of reservoir. This is due to the fact that reservoir permeability estimated in this research work using the conventional and TDS method of thermal transient testing gave 9.84 mD and 10.47 mD respectively. These values are approximately equal to the initial reservoir permeability which is 10mD.
b. It can also be used for the estimation of the initial reservoir temperature since the estimated value using pseudo reduced temperature function and the true reservoir temperature were approximately equal thus was 301.13 K and 297.04 K respectively.
c. Thermal transient testing may not be ideal for the estimation of skin factor of a reservoir since the value for the semi log and TDS thermal transient were quite far from the true reservoir value which was 10. The skin factor obtained using semi-log and TDS thermal transient testing were 2.65 and 2.85 respectively.
d. It can be said that a thorough research into thermal transient testing, it will go a long way to clarify the uncertainties in the estimating of our reservoir parameters.

6.3 Recommendations

There are other issues that came up in this research work and therefore it is recommended that;

a. An investigation is done into the effect of thermal conductivity and permeability on skin.

b. This method is can be applied to oil reservoirs in other check whether the results are reliable as the results obtained in gas reservoirs.
c. This method is used to generate type curves for the dimensionless temperature derivatives for different values of wellbore storage.
d. An investigation should be conducted on the use of the type curves generated to estimate reservoir parameters like permeability and skin factor.

REFERENCES

1. Amanat, C.,: "Pressure Buildup Analysis Technique for Oil Wells," from Gas Well testing Handbook, Elsevier science 2003.

2. Amanat, C.,: "Fundamental of Pressure Buildup Analysis Methods," from Gas Well testing Handbook, Elsevier science 2003.

3. Anh, N. D.,: "Thermal Transient Analysis Applied to Horizontal Well," paper SPE/PS/CHOA 117435 presented at SPE International Thermal Operation and Heavy Oil Symposium, held in Calgary, Alberta, October 20-23, 2003.

4. Chad, C.,: "Benefit of Conducting a Pressure Drawdown Test," from the Data Retrieval Corporation, 13231 Champion Forest Drive Suite, 401 Houston, Texas 77069, September 1, 2009.

5. Duru, O.,: "Modeling of Reservoir Temperature Transients, and Parameter estimation constrained to a Reservoir Temperature Model," pp.1-8, 2008.

6. Edwardson, M. J., Girner H. M., Parkison, Williams, C.D., Matthew C.S.,: "Calculation of formation Temperature Disturbances Caused by Mud Circulation," paper SPE 124 presented at 36th Annual Fall Meeting of SPE, Dallas, October 8-11, 1961.

7. Escobar, F.H., Hernandez, Y.A., Hernandez, C.M., "*Pressure Transient Analysis for Long Homogenous Reservoir Using TDS techniques*," Journal of Petroleum Science and Engineering, pp.68-82, 2007.

8. Escobar, F.H., Hernandez, Montealegre, M., "*Application of TDS techniques to develop Reservoir*," Journal of Petroleum Science and Engineering, pp.252-258, 2007.

9. Fan, L., Lee, W.J. Spivey, J.P.,: "Thermal Effect on Gas Well Pressure Buildup Tests: Field Application," paper SPE 55645 presented at the Rocky Mountain Regional Meeting, held in Gillette, Wyoming, May 15-18, 1966.

10. Marshall, T.R., Lie, O. H..: "A Thermal Transient Model of Circulating Wells," paper SPE 24290 presented at the SPE European Petroleum Computer Conference held in Stavanger, Norway, May 25-27, 1992.

11. Rogers, J.S., Forrest A. G., Gruy H.J.,: "A 1966 critique on Pressure transient Testing," paper SPE 1512 prepared at the 41st Annual Fall Meeting of the Society of Petroleum Engineers of AIME, held in Dallas, October 2-5, 1966.

12. Tiab, D., and Kumar, A.: "Application of PD' (Pressure Derivative) Function to Interference Analysis," Paper SPE 6053 presented at the 51st Annual Fall Meeting of the Society of Petroleum Engineers of AIME, New Orleans, LA, October 3-6, 1976. Journal of Petroleum Technology, Aug. 1980, pp. 1465-1470.

13. Tiab, D.: "Analysis of Pressure and Pressure Derivative without Type Curve Matching - I. Skin and Wellbore Storage," SPE 25426, Proceedings, SPE Prod. Oper. Symp. March 21-23, 1993, Oklahoma City, OK, 16 pages. Journal of Petroleum Science and Engr., Vol. 12, No. 3, 171-181, January, 1995.

14. Tiab, D.: "Analysis of Pressure and Pressure Derivative without Type Curve Matching - III. Vertically Fractured Wells in Closed Systems," SPE 26138, Proceedings, SPE Western Regional Meeting, May 26-28, 1993, Anchorage, Alaska, 14 pages. Journal of Petr. Science and Engr., 11, pp. 323-333, 1994.

15. Tiab, D.: "Direct Type Curve Synthesis of Pressure Transient Tests," Proceedings, SPE Rocky Mountain Conf. Denver, Colorado, March 1989, 14 pages.

16. Tiab, D.: "Analysis of Pressure and Pressure Derivative Without Type-curve Matching: 2. Vertically Fractured Wells in Closed Systems," Journal of Petr. Science and Energy. pp. 323-333, 1994.

17. Tiab, D.: '' Analysis of Pressure and Pressure Derivatives Without-Type curve Matching I-Skin and Wellbore Storage," SPE 25426 Production Operations Symposium, Oklahoma, pp. 203-216, March, 1993.

18. Tiab, D.: "Analysis of Pressure and Pressure Derivatives Without Using Type-curve Matching -Skin and Wellbore Storage," *Journal of Petroleum Science and Energy*, Vol. 12, No. 3, pp.171-181, January, 1995.

19. Wang L.W., Tamainot-Telto,R., Critoph, R.E., Metcalf, S.J.,Wang, R.Z.," Study of Thermal Conductivity, permeability, and adsorption performance of consolidated composite activated carbon adsorbent for refrigeration, "Renewable Energy, pp. 2062-2066., 2011.

20. Zhang X. M., Tong D. K.," Transient Analysis of Coalbed Methane Flow in a Coupled Reservoir-Wellbore System," School of Petroleum Engineering, China University of Petroleum, Donying 257061, China, pp. 250-254.

NOMENCLATURE

A=Cross sectional area, m^2

α= thermal diffusivity,m^2/s

C_p= heat Capacity, J/ (Kg.K)

h = height, m

k= thermal Conductivity, J/ (Kg.K)

K= permeability, mD

γ_g = Specific gravity

M= Molar Mass, g/mol

λ= constant, hr

ρ=density, kg/m^3

P_D = dimensionless Pressure

$\Delta P'_D$ = dimensionless Pressure derivative

P_{pc}= Pseudo-critical pressure, Psi

P_{pr}= Pseudo-reduced pressure, Psi

q = heat flux

R= Real gas constant, J/ (Kg.mol)

r_D = dimensionless radius

r_w= wellbore radius, m

r = reservoir radius, m

S= Skin factor

t_D = dimensionless radius

T_{pc}= Pseudo-critical temperature, K

T_{pr}= Pseudo-reduced temperature, K

T_D = dimensionless Temperature

T= Temperature, K

t = time, t

$\Delta T'_D$ = dimensionless Temperature derivative

μ= viscosity of sample, Pa s

APPENDIX A

Dimensionless Temperature data for varying dimensionless radii.

t/hr	tD	TD (rD=1)	tD*TD' (rD=1)	tD*TD' (rD=1)	TD (rD=1.1)	tD*TD' (rD=1.1)	TD (rD=1.2)	tD*TD' (rD=1.2)	TD (rD=1.3)	tD*TD' (rD=1.3)	TD (rD=1.4)	tD*TD' (rD=1.4)	TD (rD=1.5)	tD*TD' (rD=1.5)	TD (rD=2)	tD*TD' (rD=2)	TD (rD=3)	tD*TD' (rD=3)	TD (rD= 4)	tD*TD' (rD=4)	TD (rD=5)	tD*TD' (rD=5)	TD (rD=10)	tD*TD' (rD=10)	TD (rD=20)	tD*TD' (rD=20)	TD (rD=30)	tD*TD' (rD=30)	TD (rD=40)	tD*TD' (rD=40)	TD (rD=50)	tD*TD' (rD=50)
0.588	0.36	-1.22		1.98	-1.59	1.64	-1.94	1.37	-2.26	1.17	-2.55	1.01	-2.82	0.88	-3.96	0.49	-5.56	0.22	-6.70	0.12	-7.59	0.08	-10.33	0.02	-13.07	0.00	-14.68	0.00	-15.81	0.00	-16.70	0.00
0.6672	0.41	-0.97	1.98	1.98	-1.34	1.64	-1.69	1.37	-2.01	1.17	-2.30	1.01	-2.57	0.88	-3.71	0.49	-5.31	0.22	-6.45	0.12	-7.34	0.08	-10.08	0.02	-12.82	0.00	-14.43	0.00	-15.56	0.00	-16.45	0.00
0.756	0.46	-0.72	1.98	1.98	-1.10	1.64	-1.44	1.37	-1.76	1.17	-2.05	1.01	-2.32	0.88	-3.46	0.49	-5.07	0.22	-6.21	0.12	-7.09	0.08	-9.83	0.02	-12.57	0.00	-14.18	0.00	-15.32	0.00	-16.20	0.00
0.84	0.51	-0.51	1.98	1.98	-0.89	1.64	-1.23	1.37	-1.55	1.17	-1.84	1.01	-2.12	0.88	-3.25	0.49	-4.86	0.22	-6.00	0.12	-6.88	0.08	-9.62	0.02	-12.37	0.00	-13.97	0.00	-15.11	0.00	-15.99	0.00
0.912	0.56	-0.35	1.98	1.98	-0.73	1.64	-1.07	1.37	-1.39	1.17	-1.68	1.01	-1.95	0.88	-3.09	0.49	-4.70	0.22	-5.83	0.12	-6.72	0.08	-9.46	0.02	-12.20	0.00	-13.81	0.00	-14.95	0.00	-15.83	0.00
1.008	0.62	-0.15	1.98	1.98	-0.53	1.64	-0.87	1.37	-1.19	1.17	-1.48	1.01	-1.76	0.88	-2.89	0.49	-4.50	0.22	-5.64	0.12	-6.52	0.08	-9.26	0.02	-12.00	0.00	-13.61	0.00	-14.75	0.00	-15.63	0.00
1.08	0.66	-0.01	1.98	1.98	-0.39	1.64	-0.74	1.37	-1.05	1.17	-1.35	1.01	-1.62	0.88	-2.76	0.49	-4.36	0.22	-5.50	0.12	-6.38	0.08	-9.13	0.02	-11.87	0.00	-13.47	0.00	-14.61	0.00	-15.49	0.00
1.152	0.70	0.11	1.98	1.98	-0.26	1.64	-0.61	1.37	-0.92	1.17	-1.22	1.01	-1.49	0.88	-2.63	0.49	-4.23	0.22	-5.37	0.12	-6.26	0.08	-9.00	0.02	-11.74	0.00	-13.34	0.00	-14.48	0.00	-15.37	0.00
1.236	0.75	0.25	1.98	1.98	-0.12	1.64	-0.47	1.37	-0.79	1.17	-1.08	1.01	-1.35	0.88	-2.49	0.49	-4.09	0.22	-5.23	0.12	-6.12	0.08	-8.86	0.02	-11.60	0.00	-13.21	0.00	-14.34	0.00	-15.23	0.00
1.296	0.79	0.35	1.98	1.98	-0.03	1.64	-0.38	1.37	-0.69	1.17	-0.99	1.01	-1.26	0.88	-2.40	0.49	-4.00	0.22	-5.14	0.12	-6.02	0.08	-8.76	0.02	-11.51	0.00	-13.11	0.00	-14.25	0.00	-15.13	0.00
1.392	0.85	0.49	1.98	1.98	0.11	1.64	-0.23	1.37	-0.55	1.17	-0.84	1.01	-1.12	0.88	-2.26	0.49	-3.86	0.22	-5.00	0.12	-5.88	0.08	-8.62	0.02	-11.37	0.00	-12.97	0.00	-14.11	0.00	-14.99	0.00
1.512	0.92	0.65	1.98	1.98	0.27	1.64	-0.07	1.37	-0.39	1.17	-0.68	1.01	-0.95	0.88	-2.09	0.49	-3.70	0.22	-4.83	0.12	-5.72	0.08	-8.46	0.02	-11.20	0.00	-12.81	0.00	-13.95	0.00	-14.83	0.00
1.608	0.98	0.77	1.98	1.98	0.40	1.64	0.05	1.37	-0.27	1.17	-0.56	1.01	-0.83	0.88	-1.97	0.49	-3.57	0.22	-4.71	0.12	-5.60	0.08	-8.34	0.02	-11.08	0.00	-12.69	0.00	-13.82	0.00	-14.71	0.00
1.68	1.03	0.86	1.98	1.98	0.48	1.64	0.14	1.37	-0.18	1.17	-0.47	1.01	-0.74	0.88	-1.88	0.49	-3.49	0.22	-4.63	0.12	-5.51	0.08	-8.25	0.02	-10.99	0.00	-12.60	0.00	-13.74	0.00	-14.62	0.00
1.728	1.06	0.92	1.98	1.98	0.54	1.64	0.19	1.37	-0.12	1.17	-0.42	1.01	-0.69	0.88	-1.83	0.49	-3.43	0.22	-4.57	0.12	-5.45	0.08	-8.20	0.02	-10.94	0.00	-12.54	0.00	-13.68	0.00	-14.56	0.00
1.776	1.08	0.97	1.98	1.98	0.59	1.64	0.25	1.37	-0.07	1.17	-0.36	1.01	-0.63	0.88	-1.77	0.49	-3.38	0.22	-4.52	0.12	-5.40	0.08	-8.14	0.02	-10.88	0.00	-12.49	0.00	-13.63	0.00	-14.51	0.00
1.824	1.11	1.02	1.98	1.98	0.65	1.64	0.30	1.37	-0.02	1.17	-0.31	1.01	-0.58	0.88	-1.72	0.49	-3.32	0.22	-4.46	0.12	-5.35	0.08	-8.09	0.02	-10.83	0.00	-12.44	0.00	-13.57	0.00	-14.46	0.00
1.872	1.14	1.07	1.98	1.98	0.70	1.64	0.35	1.37	0.04	1.17	-0.26	1.01	-0.53	0.88	-1.67	0.49	-3.27	0.22	-4.41	0.12	-5.29	0.08	-8.04	0.02	-10.78	0.00	-12.38	0.00	-13.52	0.00	-14.41	0.00
1.92	1.17	1.12	1.98	1.98	0.75	1.64	0.40	1.37	0.09	1.17	-0.21	1.01	-0.48	0.88	-1.62	0.49	-3.22	0.22	-4.36	0.12	-5.24	0.08	-7.99	0.02	-10.73	0.00	-12.33	0.00	-13.47	0.00	-14.36	0.00
1.98	1.21	1.18	1.98	1.98	0.81	1.64	0.46	1.37	0.15	1.17	-0.15	1.01	-0.42	0.88	-1.56	0.49	-3.16	0.22	-4.30	0.12	-5.18	0.08	-7.93	0.02	-10.67	0.00	-12.27	0.00	-13.41	0.00	-14.29	0.00
2.04	1.25	1.24	1.98	1.98	0.87	1.64	0.52	1.37	0.21	1.17	-0.09	1.01	-0.36	0.88	-1.50	0.49	-3.10	0.22	-4.24	0.12	-5.12	0.08	-7.87	0.02	-10.61	0.00	-12.21	0.00	-13.35	0.00	-14.24	0.00
2.1	1.28	1.30	1.98	1.98	0.92	1.64	0.58	1.37	0.26	1.17	-0.03	1.01	-0.30	0.88	-1.44	0.49	-3.05	0.22	-4.18	0.12	-5.07	0.08	-7.81	0.02	-10.55	0.00	-12.16	0.00	-13.30	0.00	-14.18	0.00
2.16	1.32	1.36	1.98	1.98	0.98	1.64	0.64	1.37	0.32	1.17	0.03	1.01	-0.25	0.88	-1.39	0.49	-2.99	0.22	-4.13	0.12	-5.01	0.08	-7.75	0.02	-10.50	0.00	-12.10	0.00	-13.24	0.00	-14.12	0.00
2.208	1.35	1.40	1.98	1.98	1.02	1.64	0.68	1.37	0.36	1.17	0.07	1.01	-0.20	0.88	-1.34	0.49	-2.95	0.22	-4.08	0.12	-4.97	0.08	-7.71	0.02	-10.45	0.00	-12.06	0.00	-13.20	0.00	-14.08	0.00
2.256	1.38	1.44	1.98	1.98	1.07	1.64	0.72	1.37	0.40	1.17	0.11	1.01	-0.16	0.88	-1.30	0.49	-2.90	0.22	-4.04	0.12	-4.93	0.08	-7.67	0.02	-10.41	0.00	-12.02	0.00	-13.15	0.00	-14.04	0.00
2.304	1.41	1.48	1.98	1.98	1.11	1.64	0.76	1.37	0.45	1.17	0.15	1.01	-0.12	0.88	-1.26	0.49	-2.86	0.22	-4.00	0.12	-4.88	0.08	-7.63	0.02	-10.37	0.00	-11.97	0.00	-13.11	0.00	-13.99	0.00
2.352	1.44	1.53	1.98	1.98	1.15	1.64	0.80	1.37	0.49	1.17	0.19	1.01	-0.08	0.88	-1.22	0.49	-2.82	0.22	-3.96	0.12	-4.84	0.08	-7.59	0.02	-10.33	0.00	-11.93	0.00	-13.07	0.00	-13.95	0.00
2.4	1.47	1.57	1.98	1.98	1.19	1.64	0.84	1.37	0.53	1.17	0.23	1.01	-0.04	0.88	-1.18	0.49	-2.78	0.22	-3.92	0.12	-4.80	0.08	-7.55	0.02	-10.29	0.00	-11.89	0.00	-13.03	0.00	-13.91	0.00
2.64	1.61	1.75	1.98	1.98	1.38	1.64	1.03	1.37	0.72	1.17	0.42	1.01	0.15	0.88	-0.99	0.49	-2.59	0.22	-3.73	0.12	-4.61	0.08	-7.36	0.02	-10.10	0.00	-11.70	0.00	-12.84	0.00	-13.73	0.00
2.88	1.76	1.93	1.98	1.98	1.55	1.64	1.20	1.37	0.89	1.17	0.59	1.01	0.32	0.88	-0.82	0.49	-2.42	0.22	-3.56	0.12	-4.44	0.08	-7.18	0.02	-9.93	0.00	-11.53	0.00	-12.67	0.00	-13.55	0.00
3.12	1.91	2.08	1.98	1.98	1.71	1.64	1.36	1.37	1.05	1.17	0.75	1.01	0.48	0.88	-0.66	0.49	-2.26	0.22	-3.40	0.12	-4.28	0.08	-7.03	0.02	-9.77	0.00	-11.37	0.00	-12.51	0.00	-13.40	0.00
3.36	2.05	2.23	1.98	1.98	1.85	1.64	1.51	1.37	1.19	1.17	0.90	1.01	0.63	0.88	-0.51	0.49	-2.12	0.22	-3.25	0.12	-4.14	0.08	-6.88	0.02	-9.62	0.00	-11.23	0.00	-12.37	0.00	-13.25	0.00
3.6	2.20	2.37	1.98	1.98	1.99	1.64	1.65	1.37	1.33	1.17	1.04	1.01	0.76	0.88	-0.38	0.49	-1.98	0.22	-3.12	0.12	-4.00	0.08	-6.74	0.02	-9.49	0.00	-11.09	0.00	-12.23	0.00	-13.11	0.00
3.84	2.35	2.50	1.98	1.98	2.12	1.64	1.77	1.37	1.46	1.17	1.16	1.01	0.89	0.88	-0.25	0.49	-1.85	0.22	-2.99	0.12	-3.87	0.08	-6.62	0.02	-9.36	0.00	-10.96	0.00	-12.10	0.00	-12.98	0.00
4.08	2.49	2.62	1.98	1.98	2.24	1.64	1.89	1.37	1.58	1.17	1.28	1.01	1.01	0.88	-0.13	0.49	-1.73	0.22	-2.87	0.12	-3.75	0.08	-6.50	0.02	-9.24	0.00	-10.84	0.00	-11.98	0.00	-12.86	0.00
4.32	2.64	2.73	1.98	1.98	2.35	1.64	2.01	1.37	1.69	1.17	1.40	1.01	1.12	0.88	-0.01	0.49	-1.62	0.22	-2.76	0.12	-3.64	0.08	-6.38	0.02	-9.13	0.00	-10.73	0.00	-11.87	0.00	-12.75	0.00
4.56	2.78	2.84	1.98	1.98	2.46	1.64	2.11	1.37	1.80	1.17	1.50	1.01	1.23	0.88	0.09	0.49	-1.51	0.22	-2.65	0.12	-3.53	0.08	-6.28	0.02	-9.02	0.00	-10.62	0.00	-11.76	0.00	-12.64	0.00
4.8	2.93	2.94	1.98	1.98	2.56	1.64	2.22	1.37	1.90	1.17	1.61	1.01	1.33	0.88	0.19	0.49	-1.41	0.22	-2.55	0.12	-3.43	0.08	-6.17	0.02	-8.92	0.00	-10.52	0.00	-11.66	0.00	-12.54	0.00
5.28	3.22	3.13	1.98	1.98	2.75	1.64	2.40	1.37	2.09	1.17	1.79	1.01	1.52	0.88	0.38	0.49	-1.22	0.22	-2.36	0.12	-3.24	0.08	-5.99	0.02	-8.73	0.00	-10.33	0.00	-11.47	0.00	-12.35	0.00
5.76	3.52	3.30	1.98	1.98	2.92	1.64	2.58	1.37	2.26	1.17	1.97	1.01	1.69	0.88	0.55	0.49	-1.05	0.22	-2.19	0.12	-3.07	0.08	-5.81	0.02	-8.56	0.00	-10.16	0.00	-11.30	0.00	-12.18	0.00
6.24	3.81	3.46	1.98	1.98	3.08	1.64	2.73	1.37	2.42	1.17	2.12	1.01	1.85	0.88	0.71	0.49	-0.89	0.22	-2.03	0.12	-2.91	0.08	-5.66	0.02	-8.40	0.00	-10.00	0.00	-11.14	0.00	-12.02	0.00
6.72	4.10	3.60	1.98	1.98	3.23	1.64	2.88	1.37	2.56	1.17	2.27	1.01	2.00	0.88	0.86	0.49	-0.74	0.22	-1.88	0.12	-2.77	0.08	-5.51	0.02	-8.25	0.00	-9.86	0.00	-10.99	0.00	-11.88	0.00
7.2	4.40	3.74	1.98	1.98	3.36	1.64	3.02	1.37	2.70	1.17	2.41	1.01	2.13	0.88	1.00	0.49	-0.61	0.22	-1.75	0.12	-2.63	0.08	-5.37	0.02	-8.11	0.00	-9.72	0.00	-10.86	0.00	-11.74	0.00
7.68	4.69	3.87	1.98	1.98	3.49	1.64	3.15	1.37	2.83	1.17	2.54	1.01	2.26	0.88	1.12	0.49	-0.48	0.22	-1.62	0.12	-2.50	0.08	-5.24	0.02	-7.99	0.00	-9.59	0.00	-10.73	0.00	-11.61	0.00
8.16	4.98	3.99	1.98	1.98	3.61	1.64	3.27	1.37	2.95	1.17	2.66	1.01	2.38	0.88	1.24	0.49	-0.36	0.22	-1.50	0.12	-2.38	0.08	-5.12	0.02	-7.87	0.00	-9.47	0.00	-10.61	0.00	-11.49	0.00
8.64	5.28	4.10	1.98	1.98	3.72	1.64	3.38	1.37	3.06	1.17	2.77	1.01	2.50	0.88	1.36	0.49	-0.25	0.22	-1.39	0.12	-2.27	0.08	-5.01	0.02	-7.75	0.00	-9.36	0.00	-10.50	0.00	-11.38	0.00
9.12	5.57	4.21	1.98	1.98	3.83	1.64	3.49	1.37	3.17	1.17	2.88	1.01	2.60	0.88	1.46	0.49	-0.14	0.22	-1.28	0.12	-2.16	0.08	-4.90	0.02	-7.65	0.00	-9.25	0.00	-10.39	0.00	-11.27	0.00
9.6	5.86	4.31	1.98	1.98	3.93	1.64	3.59	1.37	3.27	1.17	2.98	1.01	2.70	0.88	1.57	0.49	-0.04	0.22	-1.18	0.12	-2.06	0.08	-4.80	0.02	-7.55	0.00	-9.15	0.00	-10.29	0.00	-11.17	0.00
10.08	6.16	4.40	1.98	1.98	4.03	1.64	3.68	1.37	3.37	1.17	3.07	1.01	2.80	0.88	1.66	0.49	0.06	0.22	-1.08	0.12	-1.96	0.08	-4.71	0.02	-7.45	0.00	-9.05	0.00	-10.19	0.00	-11.07	0.00
10.56	6.45	4.50	1.98	1.98	4.12	1.64	3.78	1.37	3.46	1.17	3.17	1.01	2.89	0.88	1.75	0.49	0.15	0.22	-0.99	0.12	-1.87	0.08	-4.61	0.02	-7.36	0.00	-8.96	0.00	-10.10	0.00	-10.98	0.00
11.04	6.74	4.58	1.98	1.98	4.21	1.64	3.86	1.37	3.55	1.17	3.25	1.01	2.98	0.88	1.84	0.49	0.24	0.22	-0.90	0.12	-1.78	0.08	-4.53	0.02	-7.27	0.00	-8.87	0.00	-10.01	0.00	-10.89	0.00
11.52	7.04	4.67	1.98	1.98	4.29	1.64	3.95	1.37	3.63	1.17	3.34	1.01	3.06	0.88	1.93	0.49	0.32	0.22	-0.82	0.12	-1.70	0.08	-4.44	0.02	-7.18	0.00	-8.79	0.00	-9.93	0.00	-10.81	0.00
12	7.33	4.75	1.98	1.98	4.37	1.64	4.03	1.37	3.71	1.17	3.42	1.01	3.15	0.88	2.01	0.49	0.40	0.22	-0.74	0.12	-1.62	0.08	-4.36	0.02	-7.10	0.00	-8.71	0.00	-9.85	0.00	-10.73	0.00
12.48	7.62	4.83	1.98	1.98	4.45	1.64	4.11	1.37	3.79	1.17	3.50	1.01	3.22	0.88	2.08	0.49	0.48	0.22	-0.66	0.12	-1.54	0.08	-4.28	0.02	-7.03	0.00	-8.63	0.00	-9.77	0.00	-10.65	0.00
12.96	7.91	4.90	1.98	1.98	4.52	1.64	4.18	1.37	3.86	1.17	3.57	1.01	3.30	0.88	2.16	0.49	0.55	0.22	-0.58	0.12	-1.47	0.08	-4.21	0.02	-6.95	0.00	-8.56	0.00	-9.69	0.00	-10.58	0.00
13.44	8.21	4.97	1.98	1.98	4.60	1.64	4.25	1.37	3.94	1.17	3.64	1.01	3.37	0.88	2.23	0.49	0.63	0.22	-0.51	0.12	-1.39	0.08	-4.14	0.02	-6.88	0.00	-8.48	0.00	-9.62	0.00	-10.51	0.00
13.92	8.50	5.04	1.98	1.98	4.67	1.64	4.32	1.37	4.01	1.17	3.71	1.01	3.44	0.88	2.30	0.49	0.70	0.22	-0.44	0.12	-1.33	0.08	-4.07	0.02	-6.81	0.00	-8.41	0.00	-9.55	0.00	-10.44	0.00
14.16	8.65	5.08	1.98	1.98	4.70	1.64	4.36	1.37	4.04	1.17	3.75	1.01	3.47	0.88	2.33	0.49	0.73	0.22	-0.41	0.12	-1.29	0.08	-4.03	0.02	-6.78	0.00	-8.38	0.00	-9.52	0.00	-10.40	0.00
14.4	8.79	5.11	1.98	1.98	4.73	1.64	4.39	1.37	4.07	1.17	3.78	1.01	3.51	0.88	2.37	0.49	0.76	0.22	-0.38	0.12	-1.26	0.08	-4.00	0.02	-6.74	0.00	-8.35	0.00	-9.49	0.00	-10.37	0.00
14.88	9.09	5.18	1.98	1.98	4.80	1.64	4.45	1.37	4.14	1.17	3.84	1.01	3.57	0.88	2.43	0.49	0.83	0.22	-0.31	0.12	-1.19	0.08	-3.94	0.02	-6.68	0.00	-8.28	0.00	-9.42	0.00	-10.30	0.00
15.36	9.38	5.24	1.98	1.98	4.86	1.64	4.52	1.37	4.20	1.17	3.91	1.01	3.63	0.88	2.50	0.49	0.89	0.22	-0.25	0.12	-1.13	0.08	-3.87	0.02	-6.62	0.00	-8.22	0.00	-9.36	0.00	-10.24	0.00
15.84	9.67	5.30	1.98	1.98	4.92	1.64	4.58	1.37	4.26	1.17	3.97	1.01	3.69	0.88	2.56	0.49	0.95	0.22	-0.19	0.12	-1.07	0.08	-3.81	0.02	-6.55	0.00	-8.16	0.00	-9.30	0.00	-10.18	0.00
16.32	9.97	5.36	1.98	1.98	4.98	1.64	4.64	1.37	4.32	1.17	4.03	1.01	3.75	0.88	2.62	0.49	1.01	0.22	-0.13	0.12	-1.01	0.08	-3.75	0.02	-6.50	0.00	-8.10	0.00	-9.24	0.00	-10.12	0.00
16.8	10.26	5.42	1.98	1.98	5.04	1.64	4.69	1.37	4.38	1.17	4.08	1.01	3.81	0.88	2.67	0.49	1.07	0.22	-0.07	0.12	-0.95	0.08	-3.70	0.02	-6.44	0.00	-8.04	0.00	-9.18	0.00	-10.06	0.00
17.4	10.63	5.48	1.98	1.98	5.11	1.64	4.76	1.37	4.45	1.17	4.15	1.01	3.88	0.88	2.74	0.49	1.14	0.22	0.00	0.12	-0.88	0.08	-3.63	0.02	-6.37	0.00	-7.97	0.00	-9.11	0.00	-9.99	0.00
18	10.99	5.55	1.98	1.98	5.17	1.64	4.83	1.37	4.51	1.17	4.22	1.01	3.95	0.88	2.81	0.49	1.20	0.22	0.07	0.12	-0.82	0.08	-3.56	0.02	-6.30	0.00	-7.91	0.00	-9.04	0.00	-9.93	0.00
18.6	11.36	5.62	1.98	1.98	5.24	1.64	4.90	1.37	4.58	1.17	4.29	1.01	4.01	0.88	2.87	0.49	1.27	0.22	0.13	0.12	-0.75	0.08	-3.49	0.02	-6.24	0.00	-7.84	0.00	-8.98	0.00	-9.86	0.00
19.2	11.73	5.68	1.98	1.98	5.30	1.64	4.96	1.37	4.64	1.17	4.35	1.01	4.08	0.88	2.94	0.49	1.33	0.22	0.19	0.12	-0.69	0.08	-3.43	0.02	-6.17	0.00	-7.78	0.00	-8.92	0.00	-9.80	0.00
19.92	12.16	5.75	1.98	1.98	5.38	1.64	5.03	1.37	4.71	1.17	4.42	1.01	4.15	0.88	3.01	0.49	1.41	0.22	0.27	0.12	-0.62	0.08	-3.36	0.02	-6.10	0.00	-7.71	0.00	-8.84	0.00	-9.73	0.00
20.88	12.75	5.85	1.98	1.98	5.47	1.64	5.12	1.37	4.81	1.17	4.51	1.01	4.24	0.88	3.10	0.49	1.50	0.22	0.36	0.12	-0.52	0.08	-3.27	0.02	-6.01	0.00	-7.61	0.00	-8.75	0.00	-9.63	0.00
21.6	13.19	5.91	1.98	1.98	5.54	1.64	5.19	1.37	4.87	1.17	4.58	1.01	4.31	0.88	3.17	0.49	1.57	0.22	0.43	0.12	-0.46	0.08	-3.20	0.02	-5.94	0.00	-7.55	0.00	-8.68	0.00	-9.57	0.00
22.32	13.63	5.98	1.98	1.98	5.60	1.64	5.26	1.37	4.94	1.17	4.65	1.01	4.37	0.88	3.23	0.49	1.63	0.22	0.49	0.12	-0.39	0.08	-3.13	0.02	-5.88	0.00	-7.48	0.00	-8.62	0.00	-9.50	0.00
23.28	14.22	6.06	1.98	1.98	5.68	1.64	5.34	1.37	5.02	1.17	4.73	1.01	4.46	0.88	3.32	0.49	1.71	0.22	0.58	0.12	-0.31	0.08	-3.05	0.02	-5.79	0.00	-7.40	0.00	-8.54	0.00	-9.42	0.00
24	14.66	6.12	1.98	1.98	5.74	1.64	5.40	1.37	5.08	1.17	4.79	1.01	4.52	0.88	3.38	0.49	1.77	0.22	0.64	0.12	-0.25	0.08	-2.99	0.02	-5.73	0.00	-7.34	0.00	-8.48	0.00	-9.36	0.00
26.4	16.12	6.31	1.98	1.98	5.93	1.64	5.59	1.37	5.27	1.17	4.98	1.01	4.71	0.88	3.57	0.49	1.96	0.22	0.82	0.12	-0.06	0.08	-2.80	0.02	-5.54	0.00	-7.15	0.00	-8.29	0.00	-9.17	0.00
28.8	17.59	6.48	1.98	1.98	6.10	1.64	5.76	1.37	5.44	1.17	5.15	1.01	4.88	0.88	3.74	0.49	2.13	0.22	1.00	0.12	0.11	0.08	-2.63	0.02	-5.37	0.00	-6.98	0.00	-8.11	0.00	-9.00	0.00
31.2	19.05	6.64	1.98	1.98	6.26	1.64	5.92	1.37	5.60	1.17	5.31	1.01	5.04	0.88	3.90	0.49	2.29	0.22	1.15	0.12	0.27	0.08	-2.47	0.02	-5.21	0.00	-6.82	0.00	-7.96	0.00	-8.84	0.00
33.6	20.52	6.79	1.98	1.98	6.41	1.64	6.07	1.37	5.75	1.17	5.46	1.01	5.18	0.88	4.04	0.49	2.44	0.22	1.30	0.12	0.42	0.08	-2.32	0.02	-5.07	0.00	-6.67	0.00	-7.81	0.00	-8.69	0.00
36	21.98	6.92	#NUM!	1.98	6.55	1.64	6.20	1.37	5.89	1.17	5.59	1.01	5.32	0.88	4.18	0.49	2.58	0.22	1.44	0.12	0.55	0.08	-2.19	0.02	-4.93	0.00	-6.54	0.00	-7.67	0.00	-8.56	0.00

APPENDIX B

Dimensionless Temperature data for varying skin factors

Variation of Skin			Stimulation		No Damage	Damage														
ΔT/K	t/hr	tD	tD*TD' S=-4	tD*TD' S=-2	tD*TD' S=0	tD*TD' S=2	tD*TD' S=4	tD*TD' S=6	tD*TD' S=8	tD*TD' S=10	tD*TD' S=12	tD*TD' S=14	tD*TD' S=16	tD*TD' S=18	tD*TD' S=20	tD*TD' S=22	tD*TD' S=24	tD*TD' S=26	tD*TD' S=28	tD*TD' S=30
283.65	0.588	0.36	-172.77	-109.73	-46.68	16.37	79.41	142.46	205.51	268.56	331.60	394.65	457.70	520.74	583.79	646.84	709.89	772.93	835.98	899.03
285.65	0.6672	0.41	-176.00	-112.51	-49.01	14.48	77.97	141.46	204.95	268.44	331.94	395.43	458.92	522.41	585.90	649.40	712.89	776.38	839.87	903.36
287.65	0.756	0.46	-179.23	-115.29	-51.35	12.58	76.52	140.46	204.39	268.33	332.26	396.20	460.14	524.07	588.01	651.95	715.88	779.82	843.75	907.69
289.65	0.84	0.51	-182.17	-117.79	-53.40	10.98	75.36	139.74	204.12	268.50	332.88	397.26	461.64	526.02	590.40	654.78	719.16	783.55	847.93	912.31
290.15	0.912	0.56	-183.81	-119.31	-54.82	9.67	74.16	138.65	203.15	267.64	332.13	396.62	461.11	525.60	590.10	654.59	719.08	783.57	848.06	912.56
290.95	1.008	0.62	-185.93	-121.26	-56.59	8.08	72.75	137.42	202.09	266.76	331.43	396.10	460.77	525.44	590.11	654.78	719.45	784.12	848.79	913.45
291.35	1.08	0.66	-187.30	-122.54	-57.79	6.97	71.73	136.49	201.25	266.01	330.77	395.53	460.28	525.04	589.80	654.56	719.32	784.08	848.84	913.59
292.15	1.152	0.70	-188.86	-123.93	-58.99	5.95	70.88	135.82	200.75	265.69	330.63	395.56	460.50	525.44	590.37	655.31	720.25	785.18	850.12	915.06
292.25	1.236	0.75	-190.07	-125.11	-60.15	4.81	69.76	134.72	199.68	264.64	329.60	394.56	459.52	524.47	589.43	654.39	719.35	784.31	849.27	914.23
294.15	1.296	0.79	-192.08	-126.70	-61.32	4.06	69.44	134.82	200.20	265.59	330.97	396.35	461.73	527.11	592.49	657.87	723.25	788.63	854.01	919.40
295.15	1.392	0.85	-193.91	-128.30	-62.70	2.90	68.51	134.11	199.71	265.32	330.92	396.52	462.13	527.73	593.33	658.94	724.54	790.14	855.75	921.35
296.15	1.512	0.92	-195.92	-130.10	-64.27	1.55	67.38	133.20	199.03	264.86	330.68	396.51	462.33	528.16	593.98	659.81	725.63	791.46	857.29	923.11
297.15	1.608	0.98	-197.60	-131.55	-65.50	0.54	66.59	132.64	198.69	264.73	330.78	396.83	462.88	528.93	594.97	661.02	727.07	793.12	859.16	925.21
297.65	1.68	1.03	-198.66	-132.50	-66.34	-0.18	65.98	132.14	198.30	264.46	330.61	396.77	462.93	529.09	595.25	661.41	727.57	793.73	859.89	926.04
298.15	1.728	1.06	-199.46	-133.19	-66.92	-0.65	65.62	131.89	198.16	264.43	330.70	396.97	463.24	529.51	595.78	662.05	728.32	794.59	860.86	927.13
299.15	1.776	1.08	-200.58	-134.09	-67.60	-1.10	65.39	131.88	198.37	264.87	331.36	397.85	464.34	530.83	597.33	663.82	730.31	796.80	863.30	929.79
300.15	1.824	1.11	-201.70	-134.98	-68.27	-1.55	65.16	131.88	198.59	265.31	332.02	398.74	465.45	532.16	598.88	665.59	732.31	799.02	865.74	932.45
301.15	1.872	1.14	-202.80	-135.87	-68.93	-1.99	64.94	131.88	198.82	265.76	332.69	399.63	466.57	533.50	600.44	667.38	734.31	801.25	868.19	935.12
301.65	1.92	1.17	-203.56	-136.52	-69.47	-2.42	64.63	131.68	198.72	265.77	332.82	399.87	466.92	533.96	601.01	668.06	735.11	802.16	869.20	936.25
302.15	1.98	1.21	-204.42	-137.26	-70.10	-2.94	64.22	131.38	198.54	265.70	332.86	400.01	467.17	534.33	601.49	668.65	735.81	802.97	870.13	937.29
302.35	2.04	1.25	-205.05	-137.85	-70.65	-3.44	63.76	130.96	198.17	265.37	332.57	399.78	466.98	534.19	601.39	668.59	735.80	803.00	870.20	937.41
302.65	2.1	1.28	-205.74	-138.47	-71.20	-3.93	63.34	130.61	197.88	265.15	332.42	399.69	466.96	534.23	601.50	668.77	736.04	803.31	870.58	937.85
303.15	2.16	1.32	-206.56	-139.18	-71.80	-4.41	62.97	130.35	197.73	265.11	332.49	399.87	467.26	534.64	602.02	669.40	736.78	804.16	871.54	938.93
303.55	2.208	1.35	-207.20	-139.73	-72.26	-4.79	62.68	130.15	197.62	265.09	332.56	400.03	467.50	534.97	602.44	669.91	737.38	804.85	872.32	939.79
303.95	2.256	1.38	-207.84	-140.28	-72.72	-5.16	62.40	129.96	197.52	265.08	332.64	400.19	467.75	535.31	602.87	670.43	737.99	805.55	873.11	940.67
304.35	2.304	1.41	-208.47	-140.82	-73.17	-5.52	62.12	129.77	197.42	265.07	332.72	400.37	468.01	535.66	603.31	670.96	738.61	806.25	873.90	941.55
304.75	2.352	1.44	-209.09	-141.35	-73.62	-5.88	61.86	129.59	197.33	265.07	332.81	400.54	468.28	536.02	603.75	671.49	739.23	806.97	874.70	942.44
305.15	2.4	1.47	-209.71	-141.88	-74.06	-6.23	61.60	129.42	197.25	265.07	332.90	400.73	468.55	536.38	604.20	672.03	739.86	807.68	875.51	943.33
306.15	2.64	1.61	-212.02	-143.97	-75.92	-7.87	60.18	128.23	196.27	264.32	332.37	400.42	468.47	536.52	604.56	672.61	740.66	808.71	876.76	944.80
308.15	2.88	1.76	-214.89	-146.40	-77.90	-9.41	59.08	127.57	196.07	264.56	333.05	401.55	470.04	538.53	607.02	675.52	744.01	812.50	880.99	949.49
310.15	3.12	1.91	-217.66	-148.73	-79.79	-10.85	58.09	127.02	195.96	264.90	333.84	402.77	471.71	540.65	609.58	678.52	747.46	816.40	885.33	954.27
312.15	3.36	2.05	-220.35	-150.97	-81.59	-12.21	57.18	126.56	195.94	265.32	334.70	404.09	473.47	542.85	612.23	681.61	750.99	820.38	889.76	959.14
313.15	3.6	2.20	-222.26	-152.65	-83.05	-13.45	56.16	125.76	195.37	264.97	334.58	404.18	473.78	543.39	612.99	682.60	752.20	821.80	891.41	961.01
314.15	3.84	2.35	-224.09	-154.27	-84.44	-14.61	55.21	125.04	194.87	264.69	334.52	404.34	474.17	544.00	613.82	683.65	753.48	823.30	893.13	962.96
316.15	4.08	2.49	-226.58	-156.31	-86.04	-15.77	54.50	124.77	195.04	265.31	335.58	405.85	476.12	546.40	616.67	686.94	757.21	827.48	897.75	968.02
318.15	4.32	2.64	-229.03	-158.31	-87.60	-16.88	53.83	124.55	195.26	265.98	336.70	407.41	478.13	548.84	619.56	690.27	760.99	831.70	902.42	973.14
320.15	4.56	2.78	-231.43	-160.27	-89.11	-17.95	53.21	124.37	195.53	266.69	337.85	409.01	480.17	551.33	622.49	693.65	764.81	835.97	907.13	978.29
322.15	4.8	2.93	-233.79	-162.19	-90.58	-18.98	52.63	124.23	195.83	267.44	339.04	410.65	482.25	553.86	625.46	697.07	768.67	840.28	911.88	983.48
324.15	5.28	3.22	-236.96	-164.91	-92.86	-20.81	51.24	123.29	195.33	267.38	339.43	411.48	483.53	555.58	627.63	699.68	771.73	843.78	915.83	987.87
326.15	5.76	3.52	-240.00	-167.50	-95.01	-22.52	49.98	122.47	194.96	267.46	339.95	412.44	484.94	557.43	629.93	702.42	774.91	847.41	919.90	992.39
328.15	6.24	3.81	-242.93	-169.99	-97.05	-24.11	48.82	121.76	194.70	267.64	340.58	413.51	486.45	559.39	632.33	705.27	778.21	851.14	924.08	997.02
330.15	6.72	4.10	-245.77	-172.39	-99.00	-25.62	47.76	121.15	194.53	267.91	341.29	414.68	488.06	561.44	634.82	708.21	781.59	854.97	928.36	1001.74
332.15	7.2	4.40	-248.53	-174.70	-100.88	-27.05	46.78	120.61	194.43	268.26	342.09	415.92	489.74	563.57	637.40	711.22	785.05	858.88	932.71	1006.53
334.15	7.68	4.69	-251.22	-176.95	-102.68	-28.41	45.86	120.13	194.41	268.68	342.95	417.22	491.49	565.77	640.04	714.31	788.58	862.85	937.12	1011.40
336.15	8.16	4.98	-253.86	-179.14	-104.43	-29.71	45.01	119.72	194.44	269.15	343.87	418.59	493.30	568.02	642.74	717.45	792.17	866.89	941.60	1016.32
338.15	8.64	5.28	-256.44	-181.28	-106.12	-30.96	44.20	119.36	194.52	269.68	344.84	420.00	495.17	570.33	645.49	720.65	795.81	870.97	946.13	1021.29
340.15	9.12	5.57	-258.98	-183.38	-107.77	-32.17	43.44	119.05	194.65	270.26	345.86	421.47	497.07	572.68	648.28	723.89	799.49	875.10	950.71	1026.31
342.15	9.6	5.86	-261.48	-185.43	-109.38	-33.33	42.72	118.77	194.82	270.87	346.92	422.97	499.02	575.07	651.12	727.17	803.22	879.27	955.32	1031.37
343.15	10.08	6.16	-263.17	-186.90	-110.63	-34.36	41.92	118.19	194.46	270.73	347.00	423.28	499.55	575.82	652.09	728.37	804.64	880.91	957.18	1033.45
344.15	10.56	6.45	-264.83	-188.34	-111.84	-35.35	41.15	117.64	194.14	270.63	347.13	423.62	500.12	576.61	653.10	729.60	806.09	882.59	959.08	1035.58
345.15	11.04	6.74	-266.45	-189.73	-113.02	-36.30	40.42	117.13	193.85	270.57	347.28	424.00	500.72	577.43	654.15	730.87	807.58	884.30	961.02	1037.73
346.15	11.52	7.04	-268.04	-191.10	-114.16	-37.22	39.71	116.65	193.59	270.53	347.47	424.41	501.35	578.29	655.23	732.17	809.11	886.04	962.98	1039.92
347.15	12	7.33	-269.60	-192.44	-115.28	-38.12	39.04	116.20	193.36	270.53	347.69	424.85	502.01	579.17	656.33	733.49	810.66	887.82	964.98	1042.14
348.15	12.48	7.62	-271.14	-193.75	-116.37	-38.99	38.40	115.78	193.16	270.55	347.93	425.31	502.70	580.08	657.47	734.85	812.23	889.62	967.00	1044.38
349.15	12.96	7.91	-272.65	-195.04	-117.44	-39.83	37.77	115.38	192.99	270.59	348.20	425.80	503.41	581.02	658.62	736.23	813.83	891.44	969.05	1046.65
350.15	13.44	8.21	-274.14	-196.31	-118.48	-40.65	37.18	115.00	192.83	270.66	348.49	426.32	504.14	581.97	659.80	737.63	815.46	893.29	971.11	1048.94
351.15	13.92	8.50	-275.60	-197.55	-119.50	-41.45	36.60	114.65	192.70	270.75	348.80	426.85	504.90	582.95	661.00	739.05	817.10	895.15	973.20	1051.25
352.15	14.16	8.65	-276.72	-198.45	-120.18	-41.91	36.37	114.64	192.91	271.19	349.46	427.73	506.00	584.28	662.55	740.82	819.09	897.37	975.64	1053.91
353.15	14.4	8.79	-277.84	-199.34	-120.85	-42.35	36.14	114.64	193.13	271.63	350.12	428.62	507.11	585.61	664.10	742.60	821.09	899.59	978.08	1056.58
354.15	14.88	9.09	-279.27	-200.55	-121.84	-43.12	35.60	114.32	193.03	271.75	350.47	429.18	507.90	586.62	665.34	744.05	822.77	901.49	980.21	1058.92
355.15	15.36	9.38	-280.69	-201.75	-122.81	-43.87	35.07	114.01	192.95	271.89	350.83	429.77	508.71	587.65	666.59	745.53	824.47	903.41	982.35	1061.29
356.15	15.84	9.67	-282.08	-202.92	-123.76	-44.60	34.56	113.72	192.89	272.05	351.21	430.37	509.53	588.70	667.86	747.02	826.18	905.34	984.50	1063.67
357.15	16.32	9.97	-283.47	-204.08	-124.70	-45.32	34.07	113.45	192.84	272.22	351.60	430.99	510.37	589.76	669.14	748.52	827.91	907.29	986.68	1066.06
358.15	16.8	10.26	-284.84	-205.23	-125.63	-46.02	33.59	113.19	192.80	272.41	352.01	431.62	511.22	590.83	670.44	750.04	829.65	909.26	988.86	1068.47
359.15	17.4	10.63	-286.33	-206.51	-126.68	-46.85	32.98	112.81	192.64	272.47	352.29	432.12	511.95	591.78	671.61	751.44	831.27	911.09	990.92	1070.75
360.15	18	10.99	-287.81	-207.76	-127.71	-47.66	32.39	112.44	192.50	272.55	352.60	432.65	512.70	592.75	672.80	752.85	832.90	912.95	993.00	1073.05
361.15	18.6	11.36	-289.27	-208.99	-128.72	-48.45	31.83	112.10	192.37	272.65	352.92	433.19	513.46	593.74	674.01	754.28	834.56	914.83	995.10	1075.38
362.15	19.2	11.73	-290.71	-210.21	-129.72	-49.22	31.28	111.77	192.27	272.76	353.26	433.75	514.25	594.74	675.24	755.73	836.23	916.72	997.22	1077.72
363.15	19.92	12.16	-292.25	-211.53	-130.82	-50.10	30.62	111.34	192.05	272.77	353.49	434.21	514.93	595.64	676.36	757.08	837.80	918.51	999.23	1079.95
364.15	20.88	12.75	-294.01	-213.07	-132.13	-51.19	29.75	110.69	191.63	272.57	353.51	434.45	515.39	596.33	677.27	758.21	839.15	920.09	1001.03	1081.97
365.15	21.6	13.19	-295.50	-214.34	-133.18	-52.02	29.15	110.31	191.47	272.63	353.79	434.96	516.12	597.28	678.44	759.61	840.77	921.93	1003.09	1084.25
366.15	22.32	13.63	-296.98	-215.59	-134.21	-52.83	28.56	109.94	191.33	272.71	354.10	435.48	516.87	598.25	679.63	761.02	842.40	923.79	1005.17	1086.56
367.15	23.28	14.22	-298.65	-217.04	-135.44	-53.83	27.78	109.38	190.99	272.60	354.21	435.81	517.42	599.03	680.63	762.24	843.85	925.45	1007.06	1088.67
368.15	24	14.66	-300.09	-218.26	-136.43	-54.60	27.23	109.06	190.89	272.72	354.55	436.38	518.21	600.03	681.86	763.69	845.52	927.35	1009.18	1091.01
370.15	26.4	16.12	-303.67	-221.40	-139.13	-56.85	25.42	107.69	189.97	272.24	354.51	436.79	519.06	601.33	683.61	765.88	848.16	930.43	1012.70	1094.98
372.15	28.8	17.59	-307.11	-224.40	-141.68	-58.96	23.76	106.48	189.19	271.91	354.63	437.35	520.07	602.79	685.50	768.22	850.94	933.66	1016.38	1099.09
374.15	31.2	19.05	-310.43	-227.27	-144.10	-60.94	22.22	105.39	188.55	271.71	354.87	438.04	521.20	604.36	687.52	770.69	853.85	937.01	1020.17	1103.34
376.15	33.6	20.52	-313.64	-230.03	-146.42	-62.81	20.79	104.40	188.01	271.61	355.22	438.83	522.44	606.04	689.65	773.26	856.87	940.47	1024.08	1107.69
378.15	36	21.98	-316.75	-232.70	-148.65	-64.60	19.45	103.51	187.56	271.61	355.66	439.71	523.77	607.82	691.87	775.92	859.97	944.02	1028.08	1112.13